INTEGRATED *IN SILICO* TECHNIQUES FOR MECHANISM STUDIES OF ANTIVIRAL AND ANTIDIABETIC COMPOUNDS

DIYANA BINTI MOHD ISA

FACULTY OF SCIENCE
UNIVERSITI MALAYA
KUALA LUMPUR

2020

INTEGRATED *IN SILICO* TECHNIQUES FOR MECHANISM STUDIES OF ANTIVIRAL AND ANTIDIABETIC COMPOUNDS

DIYANA BINTI MOHD ISA

DISSERTATION SUBMITTED IN FULFILMENT OF THE REQUIREMENTS FOR THE DEGREE OF MASTER OF SCIENCE

DEPARTMENT OF CHEMISTRY
FACULTY OF SCIENCE
UNIVERSITI MALAYA
KUALA LUMPUR

2020

UNIVERSITI MALAYA

ORIGINAL LITERARY WORK DECLARATION

Name of Candidate: **DIYANA BT MOHD ISA**

Matric No: **SGR140029**

Name of Degree: **MASTER OF SCIENCE**

Title of Project Paper/Research Report/Dissertation/Thesis ("this Work"): **INTEGRATED *IN SILICO* TECHNIQUES FOR MECHANISM STUDIES OF ANTIVIRAL AND ANTIDIABETIC COMPOUNDS**

Field of Study: **THEORETICAL AND COMPUTATIONAL CHEMISTRY**

I do solemnly and sincerely declare that:

(1) I am the sole author/writer of this Work;
(2) This Work is original;
(3) Any use of any work in which copyright exists was done by way of fair dealing and for permitted purposes and any excerpt or extract from, or reference to or reproduction of any copyright work has been disclosed expressly and sufficiently and the title of the Work and its authorship have been acknowledged in this Work;
(4) I do not have any actual knowledge nor do I ought reasonably to know that the making of this work constitutes an infringement of any copyright work;
(5) I hereby assign all and every rights in the copyright to this Work to the University of Malaya ("UM"), who henceforth shall be owner of the copyright in this Work and that any reproduction or use in any form or by any means whatsoever is prohibited without the written consent of UM having been first had and obtained;
(6) I am fully aware that if in the course of making this Work I have infringed any copyright whether intentionally or otherwise, I may be subject to legal action or any other action as may be determined by UM.

Candidate's Signature Date: 2 June 2020

Subscribed and solemnly declared before,

Witness's Signature Date: 2 June 2020

Name:

Designation:

INTEGRATED *IN SILICO* TECHNIQUES FOR MECHANISM STUDIES OF ANTIVIRAL AND ANTIDIABETIC COMPOUNDS

ABSTRACT

Discovery and development of drug is an iterative process that involves identification of target and leads discovery, lead optimization and pre-clinical of biological profile and is continued until the drugs are eligible to be tested in the clinical phase. Computer-aided drug design (CADD) is an efficient way to overcome the demands of cost, time consumption and drug validation. CADD utilizes *in silico* technique approaches such as molecular docking to understand their binding pattern and affinity with the target protein and molecular dynamic (MD) simulations to provide an atomic view of the dynamic behavior and stability of bioactive compound inside the target protein binding site in the aqueous solvent over a reasonable time scales. Thus, these computational techniques were able to accelerate and facilitate the drug discovery process in finding potential therapeutics lead. In this study, both methods were utilized to determine the key interaction that contributed to the optimal binding energy of antiviral and antidiabetic bioactive compounds. All compounds that were tested in *in-vitro* experiments gave a significant correlation with the computational calculation. Several residues were identified as key residues that provide significant information in improving and developing the compounds to be more potent towards the target or disease.

Keywords: drug discovery, *in silico* techniques, docking, molecular dynamic simulations

MENGINTEGRASIKAN TEKNIK *IN SILICO* UNTUK KAJIAN MEKANISME BAGI SEBATIAN ANTI VIRUS DAN ANTI DIABETIS

ABSTRAK

Penemuan dan perkembangan ubat adalah proses yang berulang termasuk pengenalan sasaran dan penemuan petunjuk, pengoptimuman petunjuk, pra-klinikal profil biologi dan diteruskan sehingga ubat tersebut layak untuk di uji pada fasa klinikal. Penemuan ubat dengan bantuan computer (CADD) adalah cara berkesan untuk mengatasi kos yang melampau, tempoh masa yang lama dan pengesahan ubat. 'CADD' menggunakan pendekatan teknik '*in silico'* seperti 'molecular docking' untuk memahami corak dan pertalian mengikat dengan protein sasaran dan simulasi dinamik molekular (MD) untuk menyediakan pandangan tingkah laku dinamik molekul dan kestabilan sebatian bioaktif pada tempat aktif protein sasaran di dalam pelarut berair pada skala masa yang tertentu. Oleh itu, teknik pengkomputeran ini dapat mempercepat dan memudahkan proses penemuan ubat dalam mencari petunjuk terapeutik yang berpotensi. Di dalam kajian ini, kedua-dua cara ini digunakan untuk menentukan kunci interaksi yang menyumbang kepada pengikat tenaga sebatian bioaktif anti-virus dan anti-diabetik. Kesemua sebatian diuji dalam eksperimen '*in vitro*' memberi korelasi yang baik dengan pengiraan pengkomputeran. Beberapa residu telah dikenal pasti sebagai kunci residu yang memberi maklumat penting dalam meningkatkan dan membangunkan sebatian menjadi lebih kuat terhadap sasaran atau penyakit.

Kata kunci: penemuan ubat, teknik *'in silico'*, 'docking', simulasi dinamik molekular

ACKNOWLEDGEMENTS

It is a pleasure to thank people who made this thesis possible and unforgettable experience for me. First and foremost, I offer my sincerest gratitude to my supervisor, Assoc. Prof. Dr. Vannajan Sanghiran Lee and my co-supervisor, Prof. Dr. Shariffudin Bin Md Zain who supported me throughout my thesis period with their enthusiasm, patience and knowledge. They provided a lot of encouragement, advises and ideas to complete my thesis.

I would like to express my sincere and heartfelt appreciation to my fellow lab mates of Computational Chemistry Laboratory Group and Drug Design and Development Research Group (DDDRG) of Chemistry Department for their good advice, comments and moral support that have been most helpful during my research project.

I also would acknowledge the collaborators, Prof. Dr. Sharmala Devi A/P K.C Sekaran and Prof. Dr. Khalijah Binti Awang for the experimental data and their constructive comments in this study. Finally, my deepest gratitude to my family for their constant support, emotional understanding and love that I received while I worked on this research project.

TABLE OF CONTENTS

LIST OF FIGURES

LIST OF TABLES

LIST OF SYMBOLS AND ABBREVIATIONS

%	:	percent
±	:	plus minus
≥	:	more than and equal to
°C	:	degree Celcius
µg/ml	:	microgram per milliliter
µM	:	microMolar
α	:	alpha
β	:	beta
2D	:	2-dimensional
3D	:	3-dimensional
Å	:	Angstrom
aa	:	amino acid
AChE	:	Acetylecholinesterase
ADMET	:	Adsorption, Distribution, Metabolism, Excretion and Toxicity
AGI	:	α-glucosidase inhibitor
AIDS	:	Acquired Immune Deficiency Syndrome
AMBER	:	Assisted Model Building and Energy Refinement
atm	:	atmospheric
C	:	Carbon
C	:	Capsid
CADD	:	Computer Aided Drug Design
CHARMm	:	Chemistry at HARvard Macromolecular Mechanics
CPS	:	Capsular Polysaccharide

CPU	:	Central Processing Unit
DENV	:	Dengue virus
DHF	:	Dengue Hemorrhagic Fever
DNA	:	Deoxyribonucleic Acid
DSS	:	Dengue Shock Syndrome
E	:	Envelope
EEL	:	Electrostatic
Eq	:	Equation
FPG	:	fasting plasma glucose
GA	:	Genetic Algorithm
GAFF	:	Generalized Amber Force Field
GPU	:	Graphics Processing Unit
H	:	Hydrogen
HDL	:	High Density Lipoprotein
HF	:	Hartree–Fock
HIV	:	Human Immunodeficiency Virus
HTS	:	High-Throughput Screening
IC_{50}	:	50% inhibitory concentration
IC_{90}	:	90% inhibitory concentration
ISI	:	Institute for Scientific Information
Kb	:	Kilobyte
K_i	:	Equilibrium Constant
LBDD	:	Ligand Based Drug Design
M	:	Molar
M	:	membrane
mABs	:	monoclonal antibodies

MC	:	Monte Carlo
MD	:	Molecular Dynamic
mg/dl	:	milligram per deciliter
MIC	:	Minimal Inhibition Concentration
MM-GBSA	:	Molecular Mechanics-Generalized Born Surface Area
mmol/l	:	millimoles per liter
MM-PBSA	:	Molecular Mechanics-Poisson-Boltzman Surface Area
N	:	Nitrogen
Na+	:	Sodium ion
nM	:	nanoMolar
NMR	:	Nuclear Magnetic Resonance
NPT	:	Number of particles, Pressure, and Temperature
NS	:	non-structural
ns	:	nanosecond
NVT	:	Number of particles, Volume, and Temperature
O	:	Oxgygen
OGTT	:	Oral Glucose Tolerance Test
oha	:	oral hypoglycaemia agent
P	:	Phosphorus
PBC	:	Periodic Boundary Condition
PDB	:	Protein Data Bank
PME	:	Particle Mesh Ewald
PMF	:	Potential Mean Force
PrM	:	pre-membrane
ps	:	picosecond
QSAR	:	Quantitative Structure Activity Relationship

RESP	:	Restrained Potential
RMS	:	Root Mean Square
RMSD	:	Root Mean Square Deviation
RMSF	:	Root Mean Square Fluctuation
RNA	:	Ribonucleic Acid
S	:	Sulphur
SDDD	:	Structure Based Drug Design
U.S	:	United State
vdW	:	van der Waal
WHO	:	World Health Organization

LIST OF APPENDICES

CHAPTER 1: INTRODUCTION

1.1 Drug discovery and development

1.1.1 Overview and challenges

Drug discovery and development is an intense and challenging process requiring multidisciplinary efforts. The process begins with the identification of target and lead followed by synthesis of lead analogs and screening to a clinical trial (Khan et al., 2013). The aim of drug discovery research is to find novel bioactive compounds that are highly specific for a given target molecule to be involved in causing disease and change the target's function (Khan et al., 2011; Shan et al., 2011; Merad et al., 2014). Hence, the ideal drugs for inhibiting specific diseases are always in great demand for the pharmaceutical industry and drug discovery research.

However, there are several challenges faced in successful discovery of ideal drugs. The process of drug discovery and development itself is demanding in terms of time consumption, cost and requires various considerations to be taken account of (Gangrade et al., 2016). According to a recent study, about 2.6 million U.S dollars were estimated to develop new drugs that gain market approval in ten years study gap (DiMasi et al., 2016). Plus, there are several unknown targets and multiple compound candidates to be screened and tested making it a complex and challenging process that would require a multi-disciplinary approach to move ahead.

Despite these challenges, there are always novel strategies to improve or hasten the process with promising drugs. Advancement in physiochemical and biological properties of molecules such as pathogenesis, diagnosis and treatment of the disease helped researches to understand the complex mechanisms involved in a specific disease (Arun, 2009). In addition, genomics, proteomics and bioinformatics technologies like crystallography and Nuclear Magnetic Resonance (NMR) provide a platform of structure

and protein target availability. The computational tools also affect various stages of drug discovery process by reducing the time and cost with minimal failure in the clinical trials phase (Bharath et al., 2011).

Utilizing all the possible approaches will lead to discoveries of novel and promising bioactive compounds in the healthcare field. The organized scientific procedure and guidelines in drug discovery helped in the improvement of drug development by which one can speed up the process and time efficiency with the help of advances in computer hardware and software.

1.2: Investigated systems

In the present work, various computational analysis of bioactive compounds from antiviral of dengue and antidiabetic will be discussed. By integrating *in silico* techniques such as molecular docking and molecular dynamic simulations, the mechanism study of binding energy and significant residues that contributed to the tight binding of putative bioactive compounds were explored together with laboratory work as references from our collaborators.

1.2.1 Antiviral of dengue

Dengue is a viral infection caused by mosquito bites that commonly cases in tropical and subtropical areas around the world. There are four serotypes of dengue virus (DENV) (Seema & Jain, 2005; Parikesit et al., 2013) and DENV-5, currently discovered in 2007 (Mustafa et al., 2015). Infection with one dengue virus serotype will stimulate an adaptive immune response that is highly cross-reactive between serotypes. Therefore, the sequential infection will increase virus replication and one is at a greater risk to develop dengue hemorrhagic fever (DHF) (Leitmeyer et al., 1999). Till now, around 2.5 billion people at risk of infection, more than 100 million cases and 25,000 deaths were reported annually (Mustafa et al., 2015). In Malaysia, a total of 124,777 dengue cases with 174

deaths were reporting in 2019 (www.who.int/docs/default-source/wpro---documents/emergency/surveillance/dengue/dengue). Thus, inhibiting all the serotypes using one inhibitor has been a great challenge in drug development for treating dengue infection. Many of the reported inhibitors are exhibiting good inhibition in targeting the wild type but not the mutants and it is much more complicated when it involved other serotypes.

Nonetheless, a number of potential proteins inhibitors have been proposed and studied. Peptides are one of the protein inhibitors that have been being improved and tested against the dengue viruses. They are one of the candidates for therapeutic agents that offer a better selectivity and specificity, predictable metabolism, with fewer side effects. However, they have poor chemical and physical stability, are rapidly cleared from the system and tend to aggregate (Skalickova et al., 2015). As previously reported, the peptide DN59 shows a promising inhibition activity against all dengue serotypes with IC_{50} of 2-5 μM in LLC-MK2 cells of DENV2. This inhibition is observed to stop viral RNA from entering the cytoplasm of the cell (Hrobowski et al., 2005; Guardia & Lleonart, 2014). The *in vitro* testing carried out by Schmidt et al. (2010a) demonstrated that a peptide derived from the stem region (residue 419 to 447) can block the viral fusion. This experiment gave a promising result for IC_{90} of 0.1-6 μM in BHK cells of DENV2.

Ever since the technology in computing advanced, computational approaches have been promoting the fast growth of the drug design process by providing prediction that saves cost and time. Recently, four designed antiviral peptides that target domain III of DENV-2 E protein by BioMoDroid algorithm was reported (Alhoot et al., 2013). Two of the peptides (DET2 and DET4) were found active in inhibiting the virus entry of DENV2. Domain III of E protein is an immunoglobin-like domain that suggested to have interaction with cellular receptors on target cells (Rey et al., 1995; Chen et al., 1997; Chiu & Yang, 2003) This virus infect the host cell via receptor mediated endocytosis followed

by fusion between endosome and virus membrane (Bressanelli et al., 2004; Modis et al., 2004; Harrison, 2008). Thus, in agreement with other studies, if an antiviral drug can interact with domain III, it is potential in blocking the virus entry stage into a host cell.

Thus, in this study, the key interacting residues of the antiviral peptides of DET2 and DET4 were identified. A comprehensive understanding on the hot spots would bring us a step closer to improve the peptides, with the possibility of inhibiting all the DENV2 was further analysed. Using Autodock Vina (Trott & Olson, 2010), a molecular docking algorithm, the complexes had generated and computed their binding affinity. Calculated binding free energy by MM-PBSA/GBSA protocol was used to differentiate the binding strength of DET2 and DET4 after molecular dynamics (MD) simulations and has been further decomposed to reveal contribution differences of the key residues that form the interactions and orient the peptides in the putative receptor binding site of the domain III. The computational findings from molecular docking and binding free energies obtained from MD simulations correlated well with the experimental results. They not only support the previous report but also provide significant details for improving the binding affinity of the peptides. Unfavourable residues identified on peptide were then replaced with other amino acids through computational site-directed mutagenesis to enhance the binding interactions. This information is crucial for future improvement and development of a better and more effective peptide inhibitor.

1.2.2 Antidiabetic of diabetes

Diabetes mellitus is a metabolic disorder described by high blood glucose rates that cause impaired in the body's ability to produce or utilize insulin. More importantly, in the long term, it will diminish the quality of a patient's life. Worldwide prevalence of diabetes in 2011 was over to 366 million and this number will be increased to approximately 552 million in 2030 (Whiting et al., 2011). Almost 3.6 million Malaysian were suffered from diabetes, the highest rate of incidence in Asia with 31.3% are adults aged 18 years and

above (The Star, 2019). The most common diabetes is type 2 diabetes mellitus where it comprises 90% of people suffering from diabetes and is caused by the body's ineffective use of insulin (American Diabetes Association, 2011).

Currently, researchers are interested to study the effective alpha glucosidase (α-glucosidase) inhibitors (AGIs) from natural sources like plant extract as an alternative for synthetic AGI to cure diabetes (Mohd Bukhari et al., 2017). This enzyme is responsible to retard overall glucose absorption by hydrolyses non-reducing 1-4 linked α-glucose terminal to release single α-glucose. The previous study reported AGI of acarbose, voglibose and miglitol are available for therapy to cure diabetes mellitus in the current market. As an example, acarbose is capable to lower the glucose absorption rate by interrupting the carbohydrate digestion and prolong the digestion time. The patients take this medicine as a tablet for oral medication three times a day and it comes with the side effects of dizziness, sweating, headache and so on (www.webmd.com/diabetes/oral-medicine-pills-treat-diabetes#1).

The plant extracts of *Nauclea subdita* (Korth.) Steud. and *Alpinia pahangensis* Ridley were isolated to investigate their activity towards the treatment of type 2 diabetes mellitus especially in inhibiting this digestive enzyme. Our collaborator was tested angustine, a major constituent in *Nauclea subdita* (Korth.) Steud., (E)-labda-8(17),12-diene-15,16-dial and zerumin A in *Alpinia pahangensis* Ridley and acarbose as a standard towards the α-glucosidase inhibitory activity. The finding showed promising activity against α-glucosidase towards angustine, which observed significantly *in vitro* enzyme inhibition of IC_{50} followed by (E)-labda-8(17),12-diene-15,16-dial and zerumin A. To further understand this process, molecular docking and dynamics simulation (MD) were performed to investigate the crucial interactions of amino acid residues between the potential ligands and target protein of α-glucosidase, 1AGM in order to find a potent drug for type 2 diabetes mellitus disease. Results suggested the calculated binding free energy

by MM-GBSA protocol of angustine could be a potential antidiabetic inhibitor against diabetes disease.

1.3 Problem statement

A series of bioactive compounds that showed inhibition activity in *in vitro* experiments towards dengue and diabetes were obtained from our collaborators. However, binding mechanism studies are lacking to support the finding in order to find the new potent drug design against these diseases together with improvement. Thus, computational approaches such as molecular docking and dynamic simulations were used to correlate the biological results by means of binding affinities and interactions.

1.4 Aim of study

This research highlights the following objectives

1. To integrate *in silico* techniques such as docking and molecular dynamic simulations for understanding the mechanism of new therapeutic drugs against dengue and diabetes disease.
2. To study the dynamics system of peptide-receptor and ligand-receptor complexes.

CHAPTER 2: LITERATURE REVIEWS

2.1 *In silico* techniques for drug discovery and development

2.1.1 History of drug discovery

In the field of medicine, drug discovery is an integrated process. The path is tedious and time consuming that also involves high cost. A statistic estimated it would take 10-12 years and up to 350 million U.S dollars to discover an ideal drug (Ooms, 2000). Moreover, only a small percentage of drug candidates will be examined in preclinical and clinical trials and few will be marketed. Thus, in consideration of production for a new drug, any advance approach in getting the drug to reach the market more quickly is needed.

Traditionally, a new drug is discovered by identifying the active compounds in traditional remedies or serendipitous discovery (Gupta, 2014). For example, aspirin is derived from the bark of willow tree (Takenaka, 2001). As time passed, emerging chemical libraries with identical or similar parent scaffold of small synthetic molecules, natural products (plants, marine, and animals) or extracts were randomly screened and tested against specific cells or complex to identify favourable activity towards the disease known as classical pharmacology (Gupta, 2014). In 1950, approximately 7 000 bioactive compounds had been isolated and synthesized for therapeutic activity testing. The challenge was more intense when 10 000 compounds had to be evaluated in 1979 and could be increased up to 20 000 compounds in present (Ooms, 2000). The high demand makes it more competitive in searching for new drugs that could be commercialized.

In the late 19th and early 20th century, the advance in analytical chemistry like chromatography, mass and NMR spectrometry (Dias et al., 2012) and purification techniques provide the extraction and characterization of active ingredients derived from medicinal plants. Morphine which is alkaloid compound was isolated from opium poppy extract in 1815 by Friedrich Wilhelm Adam Serturner (Mishra et al., 2017) and an

antibiotic of penicillin by Alexander Fleming in 1929 from penicillium mold lead (Gaynes, 2017) gave opportunities for researchers to isolate other chemically related derivatives to be new antibiotics. Development in biochemistry helped in the identification of suitable drug targets mainly from deoxyribonucleic acid (DNA), ribonucleic acid (RNA) and proteins (receptors, transporters, enzymes, and ions channels) (Baig et al., 2014).

2.1.2 Drug discovery and development process involved *in silico* techniques

As mentioned above, drug discovery and development begin with the discovery phase, optimizing phase, clinical trial phase, registration and approval by regulatory authorities. The processes are costly and time consuming but the drugs discovered or designed not only treat the infection but also have higher efficacy and give fewer side effects to patients. The *in silico* techniques used in drug discovery are more economical and accelerate the process. It helps in selecting only a potent lead to be tested and high possibility to be marketed; thereby a significant reduction in cost can be achieved (Bharath et al., 2011). In addition, they are able to access a huge amount of data generated to discover more molecules in a reliable time frame.

In silico is the Latin language which is *in silicon* means performed by using computers or via computer simulation. A mathematician, Petro Miramentos in his talk used the term '*in silico*' to define the biological experiments carried out by a computer (Gangrade et al., 2016). Figure 2.1 illustrates the *in silico* approaches involved in every stage of drug discovery and development.

Figure 2.1: *In silico* drug discovery and development process (Baig et al., 2014).

In the early stage of discovery, target was identified from DNA, RNA or other protein that are responsible for pathogenesis of the specific disease. Bioinformatics techniques help researchers to understand the protein including its evolution, phylogeny and protein modeling (Gabaldón, 2007). Protein structure prediction methods can be performed in instances such as constructing the 3D structure of target or receptor protein where 3D-crystallographic structures are not available (Gupta, 2014). The target is validated to exhibit a sufficient level of 'confident' and its relationship with the pharmacological disease of studies (Blake, 2007). Once the target was justified, potential compounds like inhibitors, modulators or antagonists for the target is determined.

The process of lead identification by ultra High-Throughput Screening (HTS) and virtual screening plays an important role in screening a large number of chemical compounds towards the target and to reduce the number of compounds to be tested in experimental studies which allow only reliable and putative compounds for lead discovery (Tang & Marshall, 2011). Pharmacophore studies are performed when one or several bioactive compounds are available and the model was built by a 3D spatial arrangement of chemical features essential for potent biological activity based on known bioactive inhibitors. Lopez-Rodriguez and co-workers (1997) successfully applied a comparative study of pharmacophore methods in the design of novel selective 5-HT4 ligands with better Ki (Ki 5-HT3 > 10 000 nM; Ki 5HT4 = 13.7 nM) in HIV treatment.

Then, the lead was optimized by structure-based drug design (SBDD) or ligand based drug design (LBDD). SBDD represents molecular docking that uses the knowledge of protein structure to select the best compounds to bind with. Successful drug design by SBDD methods is like the design of nonpeptide cyclic ureas for HIV protease and the discovery of thymidylate synthase and acetylcholinesterase (AChE) inhibitors had proved the efficiency and reliability of this analysis tool (Ooms, 2000). SBDD also helped designed Zanamivir or known as 4-guanidino-Neu5Ac2en and GG167, a potent antiviral drug towards influenza A and B viruses that are undergoing clinical phase evaluation for the influenza treatment (von Itzstein et al., 1993).

On the other hand, LBDD is an approach used when information of 3D structure was absent and relies on knowledge of molecules that interact with the biological target of interest, for example, 3D quantitative structure activity relationship (QSAR). The discovery of norfloxacin, an antibacterial inhibitor (Norrby & Jonsson, 1983) and donepezil hydrochloride, an inhibitor for Alzheimer's disease (Sugimoto et al., 2000) were assisted by QSAR analysis. *In silico* ADMET prediction gives an analysis of absorption, distribution, metabolism, excretion and toxicity of selected compounds to reduce the late failure of the pre-clinical stage. Hussain and Verma (2017) had reported that 3-(5-{[4-(aminomethyl) piperidin-1-yl] methyl}-1H-indol-2-yl)-1Hindazole- 6-carbonitrile (DB07075) compound has potent anticancer properties in terms of good docking score as well as good pharmacokinetics characteristics by docking and *in silico* ADMET analysis study. Table 2.1 illustrates the computational chemistry approaches involved *in silico* techniques.

Table 2.1: Computational chemistry approaches involved *in silico* techniques (Panigrahi and Verma, 2014).

Known protein structure	Known ligand Structure based drug design (SBDD)	Unknown ligand De novo design
Unknown protein structure	Ligand based drug design (LBDD) • 1 or more ligands (similarity searching) • Several ligands (Pharmacophore searching) • Many ligands (20+) (QSAR)	Computer aided drug design (CADD) of no use, need experimental data of some sort (HTS)

2.2 Computational methods

Nowadays, with the help of computer processing and clustering techniques advances, researches are able to perform the analysis of huge biomolecular systems at a reasonable time scale. To gain details information on the molecular and biological behavior of the compounds, computational investigation focusing on molecular docking and MD simulations were applied. The selective compounds that are potent will be docked with target protein to explore their binding conformation and energies with specific target protein that involves bioactivity testing. Then, the best ranked docked of the drug-bound complex will be subjected to MD simulations for the molecular view of the dynamics behavior inside the receptor catalytic site in an aqueous environment over a suitable time range.

Docking procedure aid initial and informative details on favourable binding modes of the drug-bound complex with the correlation of the IC_{50} in biological results if available. Even though this calculation does not give any information about the dynamic drug-receptor interactions, it provides a general description of the most favourable energy binding of ligand-bound complex conformation. In order to gain more information, MD

simulations over simulated time was performed to give further insight into the dynamic changes and stability of complex within the receptor binding site. In addition, many useful workflows for performing automation and customization in proteins and ligands system have been reported (Durrant & McCammon, 2011; Ramalho et al., 2011; Halverson et al., 2012). With computer aided advancement, it allows the process to be completed in a short time even if the complex is a large biomolecular system.

2.2.1 Molecular docking

As mentioned above, molecular docking is about calculating accurate complex interaction in terms of binding orientation and energy prediction of drug candidates to their active site of the target protein. The binding orientation or pose usually identify molecular features responsible for molecular recognition but are restricted by translational, rotational and conformational degrees of freedom. Thus, the docking algorithm helps in these challenges in finding the best matches of the docked complex. Activity prediction or scoring is achieved by the scoring functions in docking software to calculate the biological activity by estimate the interactions including van der Waals, electrostatic interaction, solvation effects and entropic effects between compound and receptor. Detailed about the type of docking, search methods and scoring functions are discussed further in this chapter.

2.2.1.1 Type of docking and search methods

There are three types of docking depending on their flexibility of protein and ligand. Rigid docking ignores the flexibility of both receptor and drug and treated like rigid molecules and had been implemented in this study. Semi-flexible docking is the situation in which protein is held fixed but the ligand is treated as flexible while flexible docking is where both ligand and protein are considered to be flexible.

Search methods are categorized into stochastic, systematic and deterministic. Stochastic methods are also known as random search methods that involve random changes of position and torsion angle to generate different conformation. The genetic algorithm (GA) and Monte Carlo algorithm (MC) are two examples of this search method. Basically, MC method generates a pool of random conformations by rotating around a bond or translational within the active site. In the case of GA, the torsion angle angles are added to chromosome (refer to position, orientation and conformation of ligand) to form new individual derivative from parents by mutation and recombination. LigandFit from Accelry's using MC as search method (Venkatachalam et al., 2003) and GOLD (Jones et al., 1995; Jones et al., 1997), AutoDock (Morris et al., 1998) and DARWIN (Taylor & Burnett, 2000) are few of docking programs using GA.

Systematic methods investigate all the degrees of freedom, both rotational and translational by utilizing fragmentation or incremental construction algorithm. For the fragmentation method, the molecules split into several rigid subparts and are docked independently and side chains are added later to rigid fragments incrementally in the active site. While incremental based approach starts with ligand fragments docked in the binding site and these fragments are ended up to be linked covalently. FlexX (Rarey et al., 1996) is applied docking software based on the incremental construction method. Deterministic methods are also known as simulation methods include molecular dynamics and mechanics methods that take an account of both ligand and protein flexibility. By the definition itself, in this approach, the initial state determines the change that can be made to generate next conformers which have relatively low energy from the initial phase.

2.2.1.2 Scoring function

Most of the docking software was implemented with a scoring function where docking score was used to rank the drugs and favourable binding interaction based on estimated

binding free energy. It divided into three categories; knowledge-based, empirical and force field based scoring function. Knowledge-based scoring functions rely on statistical means to extract rules on preferred, and nonpreferred, atom pair interactions from experimentally determined protein-ligand complexes, thus explained as pair-potential that are subsequently used to score ligand binding pose (Monika et al., 2010). Dscore (Kramer et al., 1999) and PMF score (Muegge & Martin, 1999; Muegge, 2000; Muegge, 2001) rely on this scoring function.

The empirical scoring function includes the enthalpic and entropic contribution involved in intermolecular interactions including van der Waals, electrostatic interactions and hydrogen bonds. PLP (Gehlhaar et al., 1995), ChemScore (Eldridge et al., 1997) and flexX (Rarey et al., 1996) are examples of the empirical scoring function. Force field based scoring functions estimate the binding free energy of complexes by sum of protein-ligand interaction and ligand internal energy. Different force field function depends on different sets parameter of force field, for example, Autodock (Morris et al., 1998) relies on Amber force field (Weiner & Kollman, 1981; Weiner et al., 1984; Weiner et al., 1986) and G-score (Kramer et al., 1999) on Tripos force field. In this study, CHARMm force field (Brooks et al., 1983; Nilsson & Karplus, 1986) in Accelry's was performed to calculate the enthalpy of binding.

2.2.1.3 AutoDock Vina

AutoDock Vina is a software program for molecular docking and virtual screening that assists by AutoDockTools software for the preparation of files and viewing the results. It is the successor to AutoDock 4, the most common and cited docking program in the ISI Web of Science (Sousa et al., 2006). It is faster and shown the same or improved accuracy of results analysed (Chang et al., 2010). Furthermore, AutoDock Vina is an open source that makes it feasible to access by researches for docking. However, this program has a

limitation of the maximum number of atoms, rotatable bonds and grid maps size (Trott & Olson, 2010).

For the prediction of binding affinity, empirical scoring inspired by the X-Score (Wang et al., 2002) was used. In the following paragraph, the equation and terms of the AutoDock Vina scoring function are briefly described (Quiroga & Villarreal, 2016).

The energy of binding is calculated as the sum of distance-dependent atom pair interactions (Eq.1)

$$E = \sum e_{pair}(d) \quad \text{(Eq.1)}$$

where d is the s surface distance estimate with Eq.2, as r is defined as interatomic distance and R_i and R_j are radii of the atoms in the pair.

$$d = r - R_i - R_j \quad \text{(Eq.2)}$$

Each atom connects via a steric interaction (the first three terms in Eq.3) and identical atoms pairs, hydrophobic and non-directional H-bonding interactions (the last two terms in Eq.3) is described in Eq.3.

$$e_{pair}(d) = \begin{cases} w_1 * Gauss_{\,1}(d) + \\ w_2 * Gauss_{\,2}(d) + \\ w_3 * Repulsion(d) + \\ w_4 * Hydrophobic(d) + \\ w_5 * HBond(d) \end{cases} \quad \text{(Eq.3)}$$

The steric interaction is termed using Eq.4 to 6. The combination of an attractive Gaussian function with repulsion parabolic function reproduces the general shape of a typical Lennard-Jones interaction, provided the Gaussian term is negative and the parabolic is positive. If hydrophobic atoms are involved, the linear function in Eq.7 is added. In addition, if the pair have an H-bond donor and an H-bond acceptor, Eq.8 is included.

$$Gauss_1 = e^{-((d-o_1)/s_1)^2} \quad \text{(Eq. 4)}$$

$$Gauss_2 = e^{-((d-o_2)/s_2)^2} \quad \text{(Eq. 5)}$$

$$Repulsion(d) = \begin{cases} d^2 ford \leq 0 \\ 0 ford > 0 \end{cases} \quad \text{(Eq. 6)}$$

$$Hydrophobic(d) = \begin{cases} 1 ford \leq p_1 \\ p_2 - d forp_1 > d < p_2 \\ 0 ford \geq p_2 \end{cases} \quad \text{(Eq. 7)}$$

$$HBond(d) = \begin{cases} 1 ford \leq h_1 \\ \frac{d}{-h_1} forh_1 < d < 0 \\ 0 ford \geq 0 \end{cases} \quad \text{(Eq. 8)}$$

Based on these equation, AutoDock Vina helps improve the docking abilty with good accuracy and RMSD value. With advance of C++ program and multiple CPU or CPU cores, this docking software could speed up the analysis efficiency.

2.2.2 Molecular dynamics of system

Molecular dynamic simulations (MD) are widely utilized to study biological macromolecules. It calculates the time dependent behavior of a system by providing detailed information on the protein folding, changes of conformational and fluctuation of complexes. The present computer advance accelerates and enables a large system to be simulated easily with the help of PMEMD.CUDA and GPU simulation codes. MD can be calculated based on the proposal of the study by integrating the Newton equation of motion.

A MD system is typically simulated in a solvated box to mimic the aqueous environment in biological life. The periodic boundary condition (PBC) (Adcock & McCammon, 2006) was used to handle the borders of this box. PBC is usually in

conjunction with Ewald summation methods such as particle mesh Ewald method (PME) (Darden et al., 1993). PME separates the pairwise particle-particle-interactions based on long and short range. The long-range part is treated in its Fourier transform with charge density discretized on the grid while short range part totals in real space immediately. A cut off range of 8-12 Å is normally is set to define between short and long range for both van der Waals and electrostatics interactions.

2.2.2.1 Empirical force fields

Gromos (Oostenbrink et al., 2004), Amber (Cornell et al., 1995), CHARMm (MacKerell et al., 1998) and OPLS (Jorgensen & Tirado-Rives, 1988) are the most commonly force fields used in MD (Different force fields are performed using different characteristics, for example, Gromos force field is generally used to precisely model solvation effects and Amber force fields are parameterized against ab initio data. For Amber force fields, the functional form is:

$$U(r) = \sum_{bonds} k_b(l - l_0)^2 + \sum_{angles} k_a(\theta - \theta_0)^2 + \sum_{torsions} \frac{1}{2}V_n[1 + \cos(n\omega - \gamma]$$

$$+ \sum_{i}^{N} \sum_{j>i}^{N-1} \left\{ \epsilon_{i.j} \left[\left(\frac{r_{0ij}}{r_{ij}} \right)^{12} - 2 \left(\frac{r_{0ij}}{r_{ij}} \right)^{6} \right] + \frac{q_i q_j}{4\pi\epsilon_0 r_{ij}} \right\}$$

where the potential relatively contains simple functions to describe a different type of interatomic forces. The first term (bonds) represents the energy of atoms bonded covalently, second term (angles) is energy caused by the geometry of electron orbitals involving in covalent bonding and third term (torsion) means the energy for twisting a bond by bond order and neighbouring bonds or lone pair electrons. The fourth term (*i* and *j*) is non-bonded energy of all atom pairs by vdW and ELE interactions. In this thesis, Amber force fields, ff12SB have been used for proteins and peptides that are usually the accurate models of physical forces in proteins and other biomolecules (Perez et al., 2015).

Generalized Amber force field (GAFF) was set as a force field for ligand in the diabetes case study. This force field is designed to be compatible with Amber force fields for nucleic acids and proteins, and parameterized for H, N, C, O, S, P and halogens in most small organic and pharmaceutical molecules. Both empirical and heuristic models were used to predict the force constant and partial atomic charges (Wang et al., 2004). The restrained potential charge (RESP), HF/6-31G* is set as default in GAFF parameterization (Bayly et al., 1993).

2.2.2.2 Molecular Mechanics-Poisson-Boltzmann Surface Area (MM-PBSA) and Molecular Mechanics-Generalized Born Surface Area (MM-GBSA)

MM-PBSA and MM-GBSA are approaches used to estimate the free energy of binding in MD. Basically, both methods calculate the free energy of protein-ligand complex by the following equations:

$$\Delta G_{bind} = G_{com} - (G_{rec} + G_{lig})$$

$$\Delta G_{bind} = \Delta H - T\Delta S \approx \Delta E_{MM} + \Delta G_{sol} - T\Delta S$$

$$\Delta E_{MM} = \Delta E_{internal} + (\Delta E_{electrostatic} + E_{vdw})$$

$$\Delta G_{sol} = \Delta G_{PB/GB} + \Delta G_{SA}$$

where the first term represents binding free energy of protein-ligand complex (ΔG_{bind}), complex (G_{com}), protein (G_{rec}) and ligands (G_{lig}) respectively. In the second term, (ΔG_{bind}) refer to the total energy of enthalpy (ΔH) minus the conformational entropy ($T\Delta S$) which is equivalent with enthalpy changes in the gas phase during complex formation (ΔE_{MM}) and the solvation free energy that contributed to binding (ΔG_{sol}), minus with $T\Delta S$. The third term explains molecular mechanics energy between complex in the gas phase, ΔE_{MM} as the sum of the internal energy term, ($\Delta E_{internal}$) with the electrostatic ($\Delta E_{electrostatic}$) and van der Waals energy (E_{vdw}) of protein and ligand. The

solvation energy, ΔG_{sol} can be evaluated as a sum of the polar contribution of desolvation ($\Delta G_{PB/GB}$) and non-polar contribution of desolvation (ΔG_{SA}).

The MM-PBSA model is based on the Poisson equation that enables electrostatic potential that is calculated directly from the molecular charge density in a homogeneous medium whereas MM-GBSA model based on Max Born formula for solvation energy of single ions. Both approaches give different effectiveness in terms of calculating the free energy of binding of the complex. As mentioned by Kongsted and his colleagues (2009), MM-GBSA has been experienced to perform slightly better on calculating solvation free energies on small drug-like molecules. While MM-PBSA protocol is generally applied to calculate binding affinities at reasonable computational cost with collaborative prediction of results involving both computational and experimental (Wang et al., 2018).

2.3 Antiviral for dengue

2.3.1 Overview of dengue

Dengue infection is a mosquito-borne disease caused by one of the five closely related viruses or serotypes – dengue virus (DENV) 1 to 5 (Mustafa et al., 2015) where DENV2 is the most prevalent among the serotypes. Infected female Aedes mosquitoes are the transmission vectors. Dengue is most prevalent in tropical and subtropical climates mostly in urban and semi-urban areas due to population growth and uncontrolled urbanization that becomes breeding sites for mosquitoes and leads to problems in vector control (Kyle & Harris, 2008). Incidence of dengue has grown drastically around the world in recent decades. A recent study estimated that approximately 390 million dengue infections occur per year (95% credible interval 284–528 million), of which 96 million (67–136 million) manifest clinically (with any severity of disease) (Bhatt et al., 2013). Another study had predicted that 3.9 billion people, in 128 countries, are at risk of infection with dengue viruses (Brady et al., 2012).

The WHO scheme has classified dengue virus infection into three categories; dengue fever, dengue hemorrhagic fever (DHF) and dengue shock syndrome (DSS) (www.who.int/denguecontrol/en/). Dengue fever is a severe, flu-like illness accompanied by two or more manifestations (severe headache, retro-orbital pain, muscle and joint pains, rash, swollen gland, nausea or vomiting). DHF occurs when a person meets all four clinical criteria; fever lasting 2-7 days, positive tourniquet test of hemorrhagic tendency or spontaneous bleeding, thrombocytopenia and proof of plasma leakage. DSS refers to DHF grades III and IV, in which the patient goes into shock (Gubler, 1998; Deen et al., 2006). The schematic representation of dengue classification is shown in Table 2.2.

Table 2.2: WHO classification of dengue hemorrhagic fever (Howard, 2005).

Grade	Clinical description
I	Fever with a non-specific constitutional sign of infection, only hemorrhagic symptoms
II	As for Grade I, but accompanied with more extensive hemorrhagic symptoms
III	Sign of circulatory failure or hypertension
IV	Profound shock with an undetectable pulse and blood pressure

There is no effective vaccine or antiviral drug therapy available to treat dengue due to antibody-dependent enhancement that increases the risk of dengue hemorrhagic fever or dengue shock syndrome in cases of a second exposure to a different serotype (Hotta et al., 1985; Halstead, 1988; Guy et al., 2010). Therefore, the search against dengue virus infection is an active field of research targeting different possible receptors as a potential approach to interfere with the virus.

2.3.2 Target protein of dengue

The DENV genome consists of a single, positive-strand RNA genome of 11 Kb coding that is packed by three structural proteins and a lipid bilayer (Figure 2.2) (Lindenbach, Thiel & Rice, 2007). The three structural genes are capsid (C), pre-membrane (PrM) /

membrane (M), and envelope glycoprotein (E) and seven non-structural (NS) genes (NS1, NS2A, NS2B, NS3 [protease, helicase], NS4A, NS4B, and NS5 [methyltranferase, RNA-dependent RNA polymerase]) (Baharuddin et al., 2014).

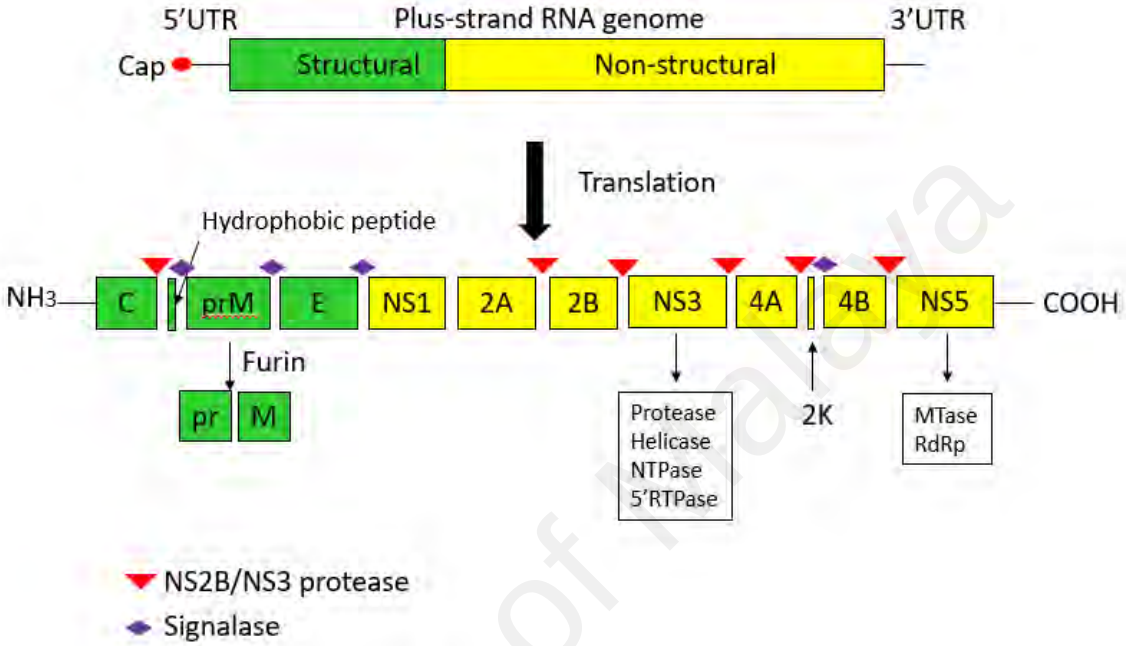

Figure 2.2: Schematic representation of flavivirus genome and polyprotein processing. Cleavage site of polyprotein by the NS2B-NS3 and host signalase are shown. The enzymatic activities of NS3 and NS5 are also indicated (Sampath & Padmanabhan, 2009).

In this study, E glycoprotein was the target protein for a potent drug against dengue where it was responsible entry of virus or cell attachment to the host receptor. It consists of three domains: a central domain (domain I), a dimerization domain (domain II) that contains hydrophobic sequences, conserved among all the flaviviruses, and the immunoglobulin-like carboxy terminal domain (domain III) (Hrobowski et al., 2005), which is responsible for cellular host binding (Watterson et al., 2012). Domain III is chosen as a potential target for inhibiting the virus's passage into the cell based on supporting evidence of (a) mutation on domain III regions caused the impaired in immune systems to neutralize the infection (Zhang et al., 2004; Modis et al., 2005; Pierson & Diamond, 2008), (b) the monoclonal antibodies able to recognize domain III region to block the infection on Vero cells (Crill & Roehrig, 2001), (c) pre-incubated cells

with soluble domain III results in significant antiviral activity, and (d) immunoglobin-like domain are seen to have interaction with cellular receptors (Rey et al., 1995; Chen et al., 1997; Chiu & Yang, 2003). The infection started with the entry of virion to the cell by endocytosis process followed by fusion between the endosome and host-cell membrane (Bressanelli et al., 2004; Modis et al., 2004; Harison, 2008). The rearrangement of E protein under acidic pH caused the fusion loop to be exposed and domain III brings the membrane closer to form fusion pores and makes RNA invade into the cytoplasm (Modis et al., 2004; Zhang et al., 2004; van der Scharr et al., 2007).

2.3.3 Antiviral peptides

Peptides are drawing increasing attention because they possess properties that bridge the gap between small molecule- and protein-based drugs. Their molecular weight ranges between a typical molecular weight of a small molecule to a protein. Peptide-based drugs also have high specificity, potency, and low toxicity/limited side effects in the biomolecular recognition processes (Röckendorf et al., 2012; Otvos & Wade, 2014). Furthermore, peptides are part of the components of the defense system found in protozoans, invertebrate, plants, and vertebrate as well as mammals that fight against invaded pathogens such as viruses, bacteria, and fungi by disrupting the orientation of their membrane (Hancock & Lehrer, 1998). A wide range of peptides has been designed and synthesized to inhibit the structural and non-structural proteins of DENV. For example, the binding of tetrapeptides (Yin et al., 2006b) and octapeptides (Prusis et al., 2013) with NS3 protease inhibits the enzymatic activity of NS3 and interferes with its interaction with NS2B (cofactor) (Falgout et al., 1993; Clum et al., 1997) that are indispensable for viral replication and maturation (Falgout et al., 1991; Zhang et al., 1992).

The development of peptide inhibitors targeting the DENV2 envelope protein is predominantly based on two approaches: high-throughput screening and mimicking peptide generation. The high-throughput screening makes use of the structural information of DENV2 envelope protein to screen randomly generated peptides (Costin et al., 2010; Schmidt et al., 2010a, 2010b). On the other hand, the generation of mimicking peptides was first reported by Hrobowski and his collages (2005). They make use of Wimley-White interfacial hydrophobicity scale in combination with known structural data to determine regions of the DENV E proteins that probably play roles in the protein-protein rearrangements or bilayer membrane interactions during the entry and fusion process (Hrobowski et al., 2005; Xu et al., 2012; Panya et al., 2015). DN59 derived specifically from the stem region of the envelope protein was shown to inhibit the DENV (Hrobowski et al., 2005; Lok et al., 2012). The rationale of deriving mimetic peptides from the E protein was further supported by a successful remark of using T20, an approved peptide for HIV treatment (Lalezari et al., 2003) that mimics part of the C-terminal region of the gp41 glycoprotein of HIV1 and inhibits the fusion of the virus to host cells (Wild et al., 1992; Chan & Kim, 1998; Kilby et al., 1998; Champagne et al., 2009). Similarly, peptides that were derived from another region of the E protein also inhibited the viral infectivity (Hrobowski et al., 2005; Costin et al., 2010). Interaction of these peptides and DENV virions led to conformational changes of the glycoproteins, causing viral RNA to be released from the viral particles (Lok et al., 2012).

2.3.4 DET1 to DET4

Previously, DET1, DET2, DET3, and DET4 have studied their antiviral activity towards DENV2 of domain III E protein. They designed based on the BioMoDroid algorithm were the calculation of the total sum of hydrophobic and charge compatibility index of domain III binding sites were taken into account. These peptides also have been evaluated in *in vitro* experiment where DET4 specifically reduces the virus' infection in

a dose-dependent manner with an IC_{50} against DENV2 of 35 μM and 84.6 % in plaque formation. The RT-qPCR analysis proved that DET2 and DET4 can lower the level of viral RNA load by blocking the virus penetrates the cell. However, DET1 and DET3 demonstrated a complete reversal of inhibition activity as they were failed to stop the virus from infecting the host cells (Alhoot et al., 2013).

2.4 Antidiabetic for diabetes

2.4.1 Overview of diabetes

Diabetes mellitus is a disease in which the blood sugar levels are too high that occurs due to the insufficiency of insulin secretion by the pancreas or due to insulin resistance. Insulin is a hormone that is responsible for glucose transport into the cell from the blood. If the production of insulin is decreased, cellular glucose uptake would be inhibited, resulting in hyperglycaemia. This high blood sugar level (hyperglycaemia) leads to long-term dysfunction, damage and even failure of vital organs such as heart, eyes, kidney, nerves and blood vessels (Shoaib et al., 2017).

Diabetes is diagnosed based on criteria of fasting plasma glucose (FPG) ≥ 7.0 mmol/l (126 mg/dl) or 2-hour oral glucose tolerance test (OGTT) ≥ 11.1 mmol/l (200 mg/dl) (Report of a WHO Consultation, 1999). After the consumption of a meal, carbohydrates are broken down into glucose and absorbed into the bloodstream leading to high blood glucose levels. So, the secretion of insulin from beta cells in the pancreas normalizes the glucose level as it enters the cell that will be used as a source of energy. Finally, the level of glucose will be low resulting in a reduction of insulin secretion. In the patient with diabetes, the absent or insufficient amount of insulin causes hyperglycaemia.

There are three main types of diabetes; type 1, type 2 and gestational diabetes. With type 1 diabetes, the body unable to produce insulin as the immune system attacks and destroy the cell in the pancreas that secretes this hormone. The most common is type 2

where the body can't utilize or secrete the insulin effectively. While, gestational diabetes appeared during pregnancy of 24th and 28th week and most women no longer have diabetes after the baby was borne (American Diabetes Association, 2010).

The first WHO global report on diabetes showed that 422 million adults are living with diabetes since 1980. The global prevalence of diabetes in 2014 among adults over 18 years of age has risen from 4.7% in 1980 to 8.5%. In 2015, diabetes was the direct cause of 1.6 million deaths and in 2012 high blood glucose was the cause of another 2.2 million deaths (www.who.int/diabetes/en/). In Asia especially Malaysia, diabetes has increased up to 20.8% and the prevalence of type 2 diabetes affecting 2.8 million individuals above the age of 30 (Zanariah et al., 2015).

It has been shown in several studies that obesity, dyslipidemia (high triglyceride and total cholesterol levels low high-density lipoprotein (HDL), and hypertension are the risk factor of diabetes disease (Kaku, 2010; Wu et al., 2014; Ley et al., 2015). Other controllable factors associated with diabetes including inactive lifestyles such as physical activity, dietary habits and smoking. However, other uncontrollable factors like genetic and ethnicity also play a significant role. Studies have shown that family history with diabetes and certain ethic and race groups are more susceptible to developing diabetes (Boulton et al., 2005). The symptoms often are not severe or may be absent such as weight loss, polyuria (increased urination), thirst and blurring of vision. Other unspecific symptoms are headache, fatigue, slow healing of cuts and itchy skin.

Type I and Type II diabetes patients can be cured by insulin therapy. It is a hormone derived either from animals or genetically from human insulin (Buysschaert et al., 2000) and responsible to treat diabetes by controlling the glucose content in the bloodstream. The hormone can be injected subcutaneously or intravenously. Other than that, oral hypoglycaemia agents (oha) are also commercially available drugs used in the treatment

of diabetes. They are sulphonylureas, Biguanides, Thiazolidindiones, Alpha (α) glucosidase inhibitors and incretineanalogues/agonists (Boulton et al., 2005). α glucosidase inhibitor (e.g. acarbose, voglibose and miglitol) for example reduces the absorption of starch, dextrins and disaccharides in the intestine and as a result, they reduce the postprandial plasma glucose.

2.4.2 Target protein for diabetes

α-glucosidase is also known as maltase, acid maltase, glucoinvertase, glucosidosucrase, lysosomal α-glucosidase and maltase-glucoamylase. It has ability to release a terminal glucose moiety from the non-reducing end of their substrates (Azam et al., 2012). This enzyme hydrolyses 1-4-linked alpha glucose residue to release a single alpha-glucose molecule and is very selective due to their subsite affinities of the active site (Chiba, 1997).

This class of enzyme has been possessed antitumor, antiviral and apoptosis-inducing activities, and some have been used in clinical settings. According to Bharatham et al. (2008), α-glucosidase was studied for AIDS treatment as a fusion target due to its dependence on the synthesis of the viral glycoproteins of glucosidase and transferase. N-butyl deoxynojirimycin, an inhibitor of the α-glucosidase was found to inhibit HIV-1 and SIVmac infectivity and tested in clinical trials (Fischer et al., 1996). This inhibitor caused the protein to be misfolded and retained within the endoplasmic reticulum and can alter glycosylation (Mehta et al., 1998).

Experimentally, various natural products had been reported as antidiabetic potentials. The medicinal plant, for example, the methanolic leaves extracts of *Terminalia* spp. showed promising activity against α-glucosidase to reduce blood glucose level (Anam et al., 2009). Ethanol extract *Garcinia daedalanthera Pierre.* leaves (Clusiaceae), *Antidesma celebicum* leaves (Euphorbiaceae), *Amaracarpus pubescens Blume.* leaves

(Rubiaceae), and *Willughbeia tenuiflora* Dyer ex Hook.f leaves (Apocynaceae) had highest *α*-glucosidase inhibition activity with IC50 of 2.33 µg/mL, 2.34 µg/mL, 3.64 µg/mL and 8,16 µg/mL compared with acarbose (117.20 µg/mL) (Elya et al., 2011). Flavonoid derivatives also exhibit excellent α-glucosidase inhibitory properties. OF2 (electron donating attached methyl derived flavonol) showed potential activity *in-vitro* enzyme inhibitors of IC_{50} of 59.96±2.09 µg/ml compared OF3 (electron withdrawing group halogen to flavonol) and OF1 (simple flavonol) with IC_{50} of 70.19±2.26 µg/ml and 71.34±1.63 µg/ml respectively (Shoaib et al., 2017).

In addition, acarbose, an α-glucosidase inhibitor is marketed as therapeutic drugs against diabetes by the suppression of carbohydrate metabolism. Carbohydrates are converted into a simple form of sugar to be absorbed through the intestine. This drug acts as a competitive and reversible inhibitor of the α-glucosidase enzyme responsible to delay carbohydrates digestion, prolong the overall time of carbohydrates digestion and thus reduces the rate of glucose absorption (Bischoff, 1995). In short term effects for a diabetes patient, this drug is capable to decrease blood sugar levels. However, their side effects include diarrhea, flatulence and malabsorption (Bray & Greenway, 1999).

2.4.3 Ligands

Plenty of work had been done on natural plant extracts to prove their potential as antihyperglycemic agents, particularly as α-glucosidase inhibitor (Manaharan et al., 2012). Plus, the phytochemicals such as flavonoids, alkaloids, terpenoids, anthocyanins, glycosides, and phenolic compounds were been observed to inhibit the enzyme activity significantly (Mohd Bukhari et al., 2017). This study will be focusing on two natural plants of *Nauclea subdita* (Korth.) Steud. and *Alpinia pahangensis* Ridley possessing α-glucosidase inhibitor activity.

2.4.3.1 *Nauclea subdita* (Korth.) Steud.

Nauclea subdita (Korth.) Steud. is naturally be found in primary forests with low altitudes − Borneo, Malaysia, Philippines and Sumatera (Catalogue of Life, 2019). In Malaysia, it is locally called as Bulobangkal, kedembak or mengkal. The tree could grow up to 25 meters and a diameter of 50 centimeters. It traditionally was used to treat the skin and to regulate menstruation (www.stuartxchange.org/Bulobangkal). Many research had suggested *Nauclea subdita* possesses antimicrobial, antioxidant, and antiproliferative properties. A study conducted by Jamaluddin et al. (2015) was showed antimicrobial activity of *Nauclea subdita* against six pathogenic microorganisms. The extract from young and matured tree was observed to inhibit both marine bacteria, *Vibrio parahaemoliticus* and *V. alginolyticus*, while *Candida albican* and *Aspergillus niger* were resistant to it. Mature trees also showed more potent zones of inhibition than young trees. The known alkaloid isolated from *Nauclea* genus, angustine has also been tested in various studies as anticonvulsant, antiproliferative, antimalarial, antimicrobial and antiparasitic properties (Takayama et al., 2003; Burn et al., 2009; Sichaem et al., 2010). Liew et al. (2012) investigate the *in vivo* vasorelaxant agent of isolated rat aorta where angustine demonstrate excellent vasorelaxant activity (more than 90% relaxation at 1×10^{-5} M) followed by nauclefine and naucletine. Angustine also one of phytoconstituents identified in the medicinal plants used in Nigeria as anti-hyperglycaemic towards diabetes (Ezuruike & Prieto, 2014).

2.4.3.2 *Alpinia pahangensis* Ridley

Alpinia pahangensis Ridley is wild ginger distributed in the lowlands forest of Pahang, Malaysia, grow up to 2 to 3 meters and traditionally used by the locals to treat flatulence. The family of Zingiberaceae, this species had been extensively studied their chemical and biological properties (Victório, 2011). Ghosh and Rangan (2013) reviewed several novel compounds extracted from the species of *Alpinia* exhibit anti-cancer, anti-inflammatory,

anti-spasmodic, anti-ulcerogenic, neuroprotective, analgesic, hepatoprotective and cardioprotective properties. The essential oils from the leaves and rhizomes of *Alpinia pahangensis* reported to inhibit five *Staphylococcus aureus* strains with minimum inhibitory concentration (MIC) values between 0.08 and 0.31 µg/µl, and four selected fungi with MIC values between 1.25 and 2.50 µg/µl (Awang et al., 2011). The rhizomes of *Alpinia pahangensis* also showed good antioxidant capacity against 5 antioxidant assays and antiproliferative activity against KB and Ca Ski cell lines (Phang et al., 2013).

The two compounds isolated from *Alpinia pahangensis,* (E)-labda-8(17),12-diene-15,16-dial and zerumin A were been reported in this study. Malek et al., (2011) investigated the cytotoxic effects of (E)-labda-8(17),12-diene-15,16-dial against six human cancer cell lines including lung, colon and breast tumor cell lines. Other than this, (E)-labda-8(17),12-diene-15,16-dial also shows antibacterial, antiprotozoal, antifungal, antitubercular, antioxidant and anti-inflammatory activity (Richomme et al., 1991; Habibi, et al., 2000; Kirana et al., 2003; Yunbao & Muraleedharan, 2010). Additionally, (E)-labda-8(17),12-diene-15,16-dial, the major constituent of mango ginger showed a high α-glucosidase inhibition slightly less than the commercial product, acarbose (Yoshioka et al., 2019). While zerumin A demonstrated strong antimicrobial activity against *Escherichia coli* with an inhibition zone diameter of 20 mm at 20 µg bacterial concentration studied by Sheeja and Nair (2014). A recent study revealed the α-glucosidase inhibitory activity to assess the anti-diabetes properties of Zerumin A with IC_{50} values of 1.55 ± 0.42 (Awin et al., 2020).

CHAPTER 3: METHODOLOGY

3.1 Integrated *in silico* techniques for mechanism study of antiviral compounds

3.1.1 Docking studies

The PDB code of 2JSF, DENV2 E protein of domain III was used as a target receptor (Volk et al., 2007) and optimized with CHARMm force field with Momany-Rone partial charge (Momany & Rone, 1992) in Discovery Studio 2.5.5. The peptide structures (DET1 to DET4) (Alhoot et al., 2013) were subjected to peptide tertiary structure server that designed the structures based on information of β-turns and regular secondary structure states (Kaur et al., 2007). Then, all the structures prepared were minimized until Root Mean Squared (RMS) gradient tolerance of 0.1000 (kcal mol^{-1} x Å) is satisfied. The docked structures obtained from AutoDock Vina (Trott & Olson, 2010) with the grid box build of 30 × 30 × 30 size and grid spacing is 1 to cover the position of the amino acid of 92 to 101 (IGVEPGQLKL), which was previously defined as the binding site of the protein in the lateral loop of domain III (Hung et al., 2004; Mazumder et al., 2007) were performed. The properties of peptides were predicted by peptide property calculator from pepcalc.com (www.pepcalc.com/).

3.1.2 Molecular dynamic simulations and binding free energy calculation

Molecular dynamics (MD) simulation protocol were prepared from AMBER 12 program by using PMEMD.CUDA (Götz et al., 2012; Grand et al., 2013; Salomon-Ferrer et al., 2013). All docked complex has subsequently been solvated in TIP3P water of cubic box extending 15 Å to compute the non-bonded interactions. AMBER 12 force field (ff12SB) (Case et al., 2012) was applied to the system and sodium ions (Na+) as the counterion was randomly added to neutralize the complex. The whole MD simulation process was performed under periodic boundary conditions (Weber et al., 2000) and the Particle-Mesh-Ewald (PME) method (Darden et al., 1993; Essmann et al., 1995). The

bonds that involve hydrogen were constrained and the temperature was controlled by the SHAKE algorithm and Langevin dynamics. For over 60 picoseconds (ps) of NVT (constant Number of particles, Volume, and Temperature) dynamics, the temperature was increased constantly from 0 to 37 °C, followed by NPT (Number of particles, Pressure, and Temperature) equilibration of 300 ps. Finally, a production stage of 15 nanoseconds (ns) MD simulation run were conducted (Kodchakorn et al., 2014). However, for modified peptides, only 10 ns of the simulated time were performed.

Trajectories analyses of root mean square deviation and fluctuation and hydrogen bonds were carried out using the CPPTRAJ package from Amber 12 (Roe & Cheatham, 2013). Calculated binding free energy of each system were computed by MM-PBSA (Molecular Mechanics-Poisson-Boltzmann Surface Area (Kollman et al., 2000) and MM-GBSA (Molecular Mechanics-Generalized Born Solvent Area methods (Chong et al., 1999) protocol using 500 snapshots from MD trajectories of 11 to 15ns. Whereas, in the case of the modified peptide, the MM-PBSA methods and trajectories of 6 to 10 ns were used to analyse the complex binding interaction. All the images were generated using PyMOL version 1.6.

3.1.3 Energy calculation and mutation study

BeAtMuSiC (Dehouck et al., 2013) is a webserver predictor based on coarse-graining of the changes in the binding free energy of protein-protein interactions induced by the point mutations. It relies on a set of statistical potentials derived from known protein structures and combines the effect of the mutation on the strength of the interactions at the interface as well as on the overall stability of the complex. The server provides all possible mutations in a protein chain or at the interface rapidly, with the best predictive performance. The snapshots of our previously simulated complex of DET4 and domain III at every ns (1 to 15 ns) were uploaded to the server while the changes in the binding free energy resulted from each suggested mutation were obtained. The unfavourable

residues of DET4 (ALA118, GLY123, LYS124, LEU125, ASP126 and PHE127) were then mutated to the suggested amino acids with the lowest binding free energy value by the BeAtMuSiC server, followed by the 10 ns of molecular dynamics (MD) simulations.

Amino acid substitution matrix is a matrix of preferred amino acid exchange that provides "safe" amino acid substitutions i.e. least likely to disturb the protein folding structure, allowing the probing of the structural and functional significance of the substituted site (Bordo & Argos, 1991). The matrix suggests substitution candidates on unfavourable residue, (e.g. GLY prefers ASN as the most desirable charged or polar substituent), based on certain criteria such as buried residue, exposure of certain amino acids beyond some water-accessible surface threshold, and other cases, regardless of the accessible state.

3.2 Integrated *in silico* techniques for mechanism study of antidiabetic compounds

3.2.1 Molecular docking

The three-dimensional structure of α-glucosidase bound with acarbose complex from *Aspergillus awamori* with 2.4 Å resolution, 1AGM (Aleshin et al., 1994) has been determined as target protein in this study. All waters and ligands were being removed and modified based on the CHARMm force field with partial charge Momany-Rone (Momany & Rone, 1992) followed by short minimizations in Discovery Studio 2.5.

The ligands, angustine, (E)-labda-8(17),12-diene-15,16-dial, zerumin A and acarbose (Figure 3.1) that had been tested *in vitro* by the collaborator were downloaded at the PubChem compound server and optimized based on functional B3LYP, the basis set of 6-31G* (d,p) in Gaussian 09 (Frisch et al., 2016) before minimized with the same protocol as for target protein. AutoDock Vina (Trott & Olson, 2010) program was used for rigid docking of ligands into the binding site (ARG52, ASP53, LEU174, GLU176, ARG301, and GLU395) (Aleshin et al., 1994) of the target protein. The polar hydrogen atoms were

added and nonpolar hydrogen atoms were merged in preparation of ligands by AutoDock Tools 4.2 (Morris et al., 2009). The grid box of 40 × 40 × 40 sizes and grid spacing of 1 were set up to cover the entire binding active site of receptors. All conformation of ligand-bound complexes were analysed in term of binding affinity.

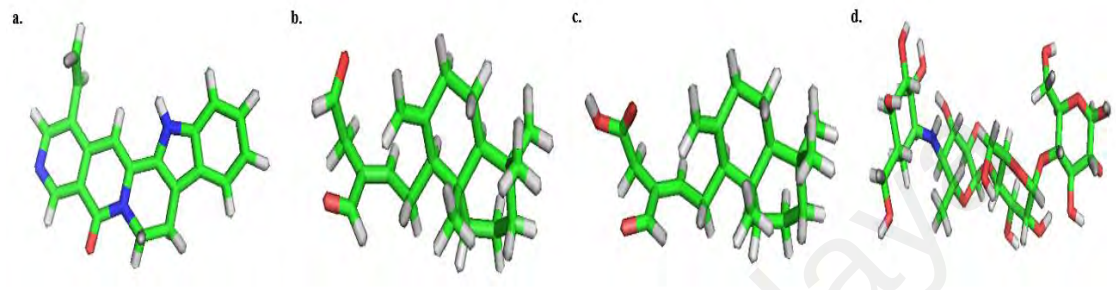

Figure 3.1: 3D structures of minimized ligands in stick representation. a. angustine, b. (E)-labda-8(17),12-diene-15,16-dial, c. zerumin A and d. acarbose.

3.2.2 Molecular dynamic simulations and binding free energy analysis

Two active compounds (angustine and (E)-labda-8(17),12-diene-15,16-dial) and standard, acarbose were selected for MD simulation by PMEMD.CUDA (Götz et al., 2012; Grand et al., 2013; Salomon-Ferrer et al., 2013) from AMBER 12 on GPUs Quadro 2000D produced by NVIDIA which speeds up the simulation wall time required to obtain the trajectory files from each simulation.

Before that, ligands were sent to RESP ESP charge derive server to generate force field parameter and build force field library (Vanquelef et al., 2011). The force field of GAFF from antechamber module (Wang et al., 2004) was applied to ligands. Then, the complex was solvated at least 10 Å extending in each direction from protein surface in a cubic box of TIP3P water where the force field 12 (ff12SB) (Case et al., 2012) were applied. To neutralize, sodium ions (Na+) as counterion were added to the protein-ligand complex and the cut-off radius was kept to 20 Å to compute the nonbonded interactions. All simulations were performed under the same condition as described in previous MD simulation protocols and 10 ns production of MD trajectories were collected to analyse

using the PTRAJ module of the amber package. A total of 500 snapshots from the last 5ns trajectories of the simulation were subjected to SANDER module in Amber 12 to compute the complex interaction energy profiles based on MM-PBSA (Kollman et al., 2000) and MM-GBSA (Chong et al., 1999).

CHAPTER 4: RESULTS AND DISCUSSION

4.1 *In silico* screening for mechanism study of antiviral compounds

4.1.1 Dockings of designed peptides at domain III

Based on experimental results by Alhoot and his co-worker (2013), the designed peptides of DET1, DET2, DET3 and DET4 were selected to study their binding mechanism towards domain III E protein of DENV2. A docking study was been carried out to predict the binding energy profiles of these peptides on the DENV2 envelope protein domain III. The designed peptide structures were generated by peptide tertiary structure prediction server (Kaur et al., 2007) were illustrated in Figure 4.1. All four peptides were bound to the surface of domain III as this region was identified as receptor attachment of DENV into the cell with DET4 was seen to be nearest to the binding site of position 92-IGVEPGQLKL-101 residues (Hung et al., 2004; Mazumder et al., 2007) (Figure 4.2). The estimated binding affinity range of -9.6 kcal mol^{-1} to -7.2 kcal mol^{-1} (Table 4.1) revealed the favourable interactions of peptide-bound complexes. The results from docking proved DET4 outperformed than other peptides and appeared to be the most active peptide that binds to the target protein. Predicted binding affinities were calculated for DET1- and DET3-bound complex for confirmation of experimental data correlation.

Table 4.1: Molecular docking results of DET-bound complex from AutoDock Vina.

Target	Peptide	Sequence	Inhibition (% μM)	Binding Affinity (kcal mol^{-1})
2JSF	DET1	GWVKPAKLDG	0	-7.2
	DET2	PWLKPGDLDL	40.6	-9.0
	DET3	IGVRPGKLDL	0	-7.2
	DET4	AGVKDGKLDF	84.6	-9.6

Note: Inhibition percentage was retrieved from reference (Alhoot et al., 2013)

Table 4.2 shows the properties of DET1 to DET4 calculated from pepcalc.com (www.pepcalc.com/). All four peptides exhibit both positive and negative charged and hydrophobic residues (polar residues are not found) with good solubility in the water. DET1 and DET3 are basic, while DET2 and DET4 are acidic and neutral, respectively.

Although all the peptides are similar to one another (with a similar portion of hydrophobic and charged residues), DET4 is the only neutral peptide without proline, while DET2 is the only peptide with one glycine and two prolines. Proline is known to rigidify the polypeptide chain by imposing certain torsion angles on the segment of the structure and glycine contributes high flexibility of a polypeptide chain. The attributes of the peptides probably influence the binding ability of the peptide at the binding site. As observed, DET4 with no proline (no rigid/constraint structure) and extra charged-residues compared to others bind better to the binding site.

Table 4.2: Peptides properties.

Peptide	Sequence	Molecular weight	Iso-electric point	Net charge at pH 7	Estimated solubility
DET1	GWVKPAKLDG	1070.2	9.9	1 (basic)	Good
DET2	PWLKPGDLDL	1153.3	3.7	-1 (acidic)	Good
DET3	IGVRPGKLDL	1067.3	10.1	1 (basic)	Good
DET4	AGVKDGKLDF	1049.2	6.8	0 (neutral)	Good

Red: acidic residues, blue: basic residues, green: hydrophobic uncharged residues, black: other residues. Molecular weight is in the unit of g/mol.

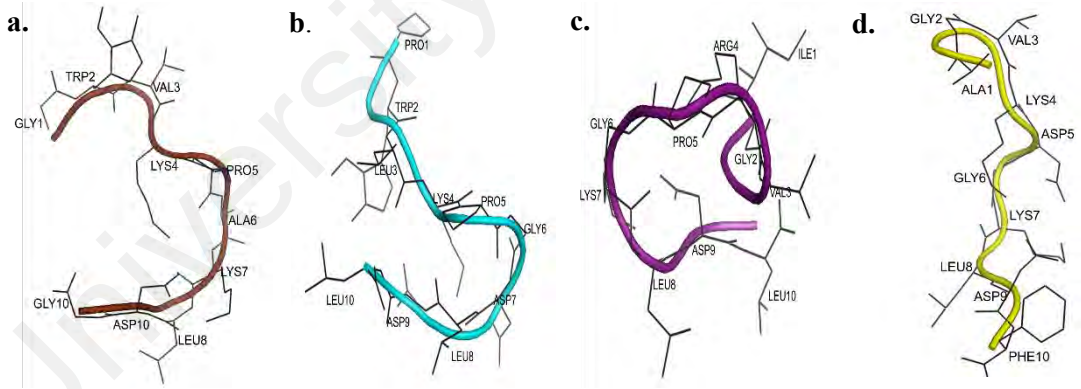

Figure 4.1: Tertiary structure of the peptides (initial and minimized structures). a. DET1, b. DET2, c. DET3, and d. DET4. The peptides are shown in line representation (initial structures from the prediction server are shown in black) and the optimized peptide structures are shown in cartoon representation.

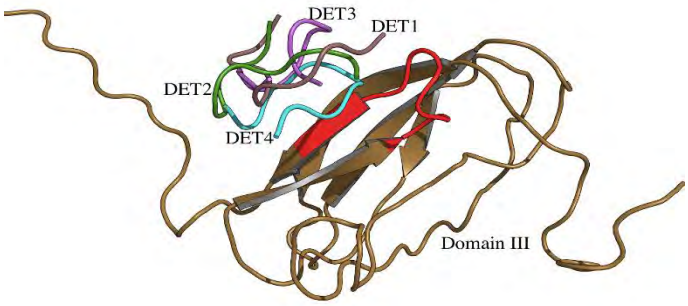

Figure 4.2: Docked conformations of DET1 to DET4 at the binding site of DENV2 envelope protein domain III (brown). All peptides are bound on the surface of domain III, at the immediate vicinity of the binding site (red), with DET4 (cyan) being the nearest to the binding site.

4.1.2 Molecular dynamic simulations

4.1.2.1 System stability and flexibility

The structural stability of the systems is monitored using root mean square deviations (RMSD) of all Cα-atoms with respect to their minimized starting structure. From the plotted graph (Figure 4.3), the starting structure of the DET4-bound complex was observed to have a higher RMSD value but eventually ascend steadily with acceptable range of fluctuation compared to the DET2-bound complex. This indicates the DET4-bound complex has reached equilibrium and stable within the simulated timescale and reflects the instability of structural changes in the DET2-bound complex especially at 9 to 11 ns (Figure 4.3). The root mean square fluctuations (RMSF) of the last 5ns simulation was also computed and plotted (Figure 4.4). RMSF is useful to identify or locate the flexible/disordered region as well as the heterogeneity of a system (Król et al., 2005; Yin et al., 2006a; Sousa et al., 2009). DET2-bound complex shows a greater RMSF value compared to the DET4-bound complex, especially in the peptide region (residues 118 to 127), demonstrated that DET2 fluctuates more and struggle to find conformation to be fit in the binding pocket or is probably unstable in the binding pocket (Figure 4.4). Whilst, binding of DET4 stabilizes the complex as a whole and results in a reduced fluctuation (for the peptide and protein). A similar trend was seen in the snapshots of the complex

conformation at 11, 12, 13, 14, and 15 ns where DET2 tries to bind stably with domain III, compared to DET4 (Figure 4.5). This is also in agreement with the RMSD calculation, where smaller deviations for protein in complex with DET4 are observed (Figure 4.3).

Figure 4.4 indicates that residues at the N- and C- terminus of the peptides show higher fluctuations, i.e. PRO and ALA at position 118 in DET2 and DET4, respectively, and LEU and PHE at position 127. These residues also show a less favourable/positive interaction energy from the decomposition energy (see the section below). This is also observed in TRP119, LEU125, and ASP126 of DET2, and LYS124, LEU125, and ASP126 of DET4. The binding site of the domain III (residue 92 to 101) shows a relatively low RMSF (Figure 4.4, shaded region), except for GLU95 and PRO96, for DET2- and DET4-bound system, respectively. These residues corresponded to the less favourable/positive interaction energy, as shown by the decomposition analysis.

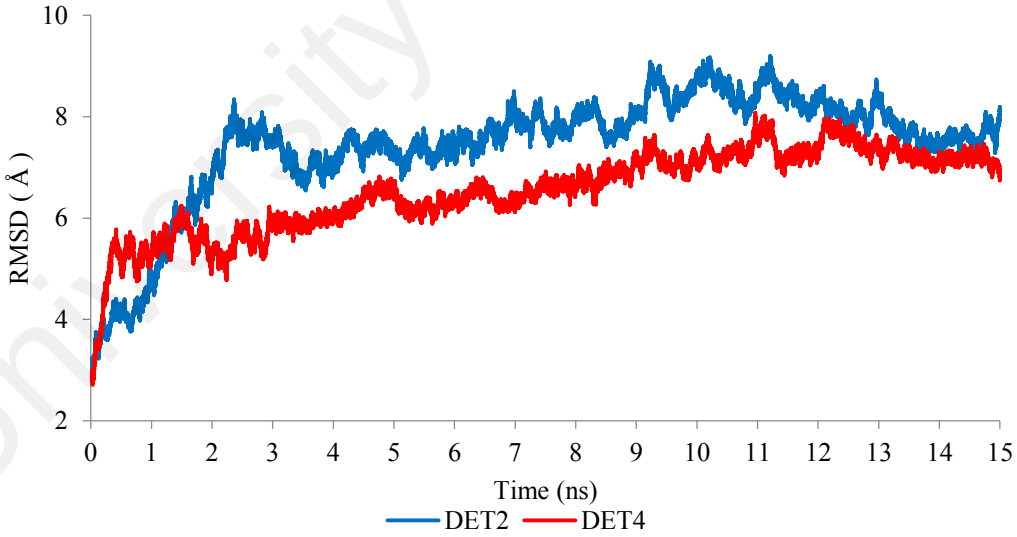

Figure 4.3: Root mean square deviations (RMSD) of all Cα-atoms of DET2- and DET4-bound systems along the 15 ns simulation time.

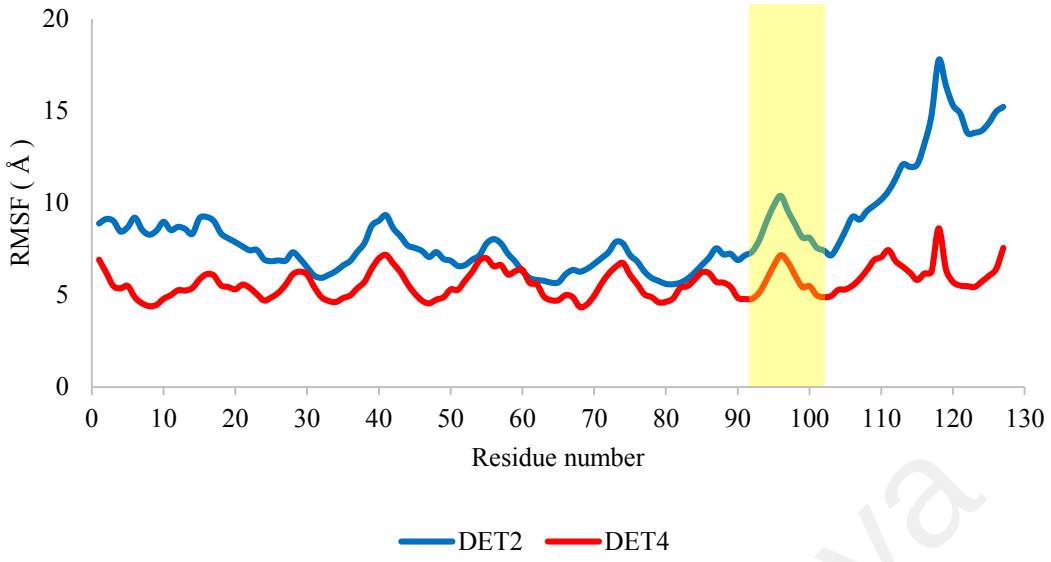

Figure 4.4: Root mean square fluctuations (RMSF) of DET2- and DET4- bound systems, calculated for every residue of the domain III (residue 1-117) and the peptides (residue 118-127), separated by a vertical line. The binding site of the domain III (residue 92 to 101) is shaded in yellow.

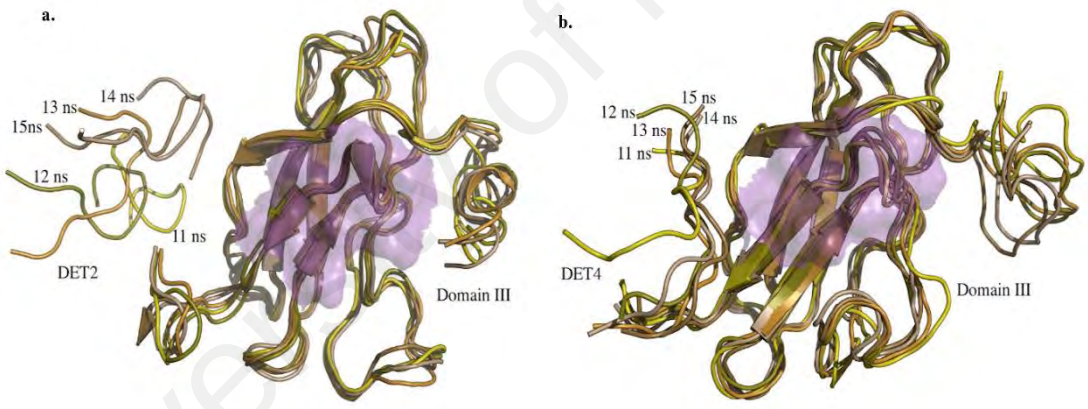

Figure 4.5: Snapshots of a. DET2- and b. DET4- bound complexes at 11-15 ns. The binding site is shown in purple surface. DET4 binds closer to the binding site and remains at the site throughout the simulations, as compared to DET2. For clarity, the loop at the C-terminal region is not shown.

4.1.2.2 Binding free energy calculation

The MM-PBSA/GBSA approaches were used to estimate the binding free energy of complexes. Based on ΔE calculated values, both methods gave correlated value with previous experimental findings, where the inhibition activity of DET4 is higher than DET2 by a factor of 2 (Alhoot et al., 2013). However, a recent study had suggested that MM-PBSA yields the best correlation between the predicted binding affinities and the

experimental data for protein-peptide and protein-protein interaction (Weng et al., 2019). The relative binding free energy obtained from MM-PBSA calculation proved that DET4 binds to the protein better than DET2 (-26.80 kcal mol^{-1} versus -13.81 kcal mol^{-1}) (Table 4.3). The van der Waals (vdW) interactions and non-polar parts of the solvation free energy contribute favourably to the binding, as opposed to the unfavourable total electrostatic contributions (ΔG_{sol}) (Table 4.3). Each energy terms were found to be at least two times more favourable upon the binding of DET4, compared to that for DET2, e.g. -36.03 kcal mol^{-1} versus -16.07 kcal mol^{-1} for the vdW interactions.

Table 4.3: Relative binding free energies of DET-bound complexes estimated using MM-PBSA/GBSA.

Energy term	DET2-bound complex (kcal mol^{-1})	DET4-bound complex (kcal mol^{-1})
EEL	-93.70 ± 30.14	-175.72 ± 46.59
vdW	-16.07 ± 3.58	-36.03 ± 4.43
$\Delta G_{sol\ (MM-PBSA)}$	95.95 ± 29.67	184.95 ± 47.74
$\Delta G_{sol\ (MM-GBSA)}$	102.80 ± 30.03	198.23 ± 46.86
$\Delta E_{MM-PBSA}$	-13.81 ± 3.37	-26.80 ± 5.22
$\Delta E_{MM-GBSA}$	-6.96 ± 2.56	-13.52 ± 3.53

Note: The EEL and vdW represent the electrostatic and van der Waals contributions from MM, respectively. ΔGsol $_{(MM-PBSA/GBSA)}$ stands for electrostatic and nonpolar contribution to the solvation energy. $\Delta E_{MM-PBSA/GBSA}$ (in kcal mol^{-1}, binding energy neglecting the contribution of entropy) is the final estimated binding free energy calculated.

To identify the important amino acids that contribute to the binding affinity, per residue energy decomposition were calculated for DET2- and DET4-bound complexes. Figure 4.6 to Figure 4.8 illustrates the decomposed energies on a per residue basis for the key binding residues in the peptides (DET2 and DET4) and the protein (domain III). The positive and negative values indicate unfavourable and favourable contributions, respectively. Several residues were identified to have significant contributions more than 1.00 kcal mol^{-1} to the binding – LEU120 and PRO122 from DET2, and GLY119, VAL120, LYS121, and ASP122 from DET4 (Figure 4.6 and Figure 4.7), implicating that these residues are important in holding the peptide in place in the binding pocket via favourable peptide-protein interactions. Figure 4.8 shows the decomposition binding

energy upon the binding of DET2 and DET4 on domain III. DET4 has contact with all the residues in the binding site compared to DET2, where LEU101 contributes the most. The small contributions from the binding site indicate that DET2 and DET4 had probably drifted away from the binding site, especially for the case of DET2. However, the DET4-bound complex remained more stable compared to the DET2-bound complex (Figure 4.5).

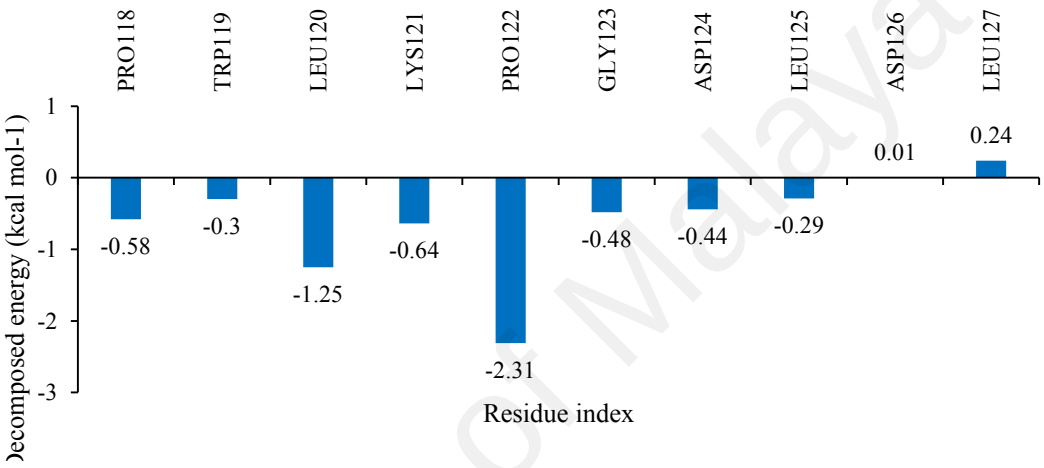

Figure 4.6: Decomposed binding free energy (kcal mol^{-1}) of DET2 on a per residue basis during 11-15 ns of the simulation time.

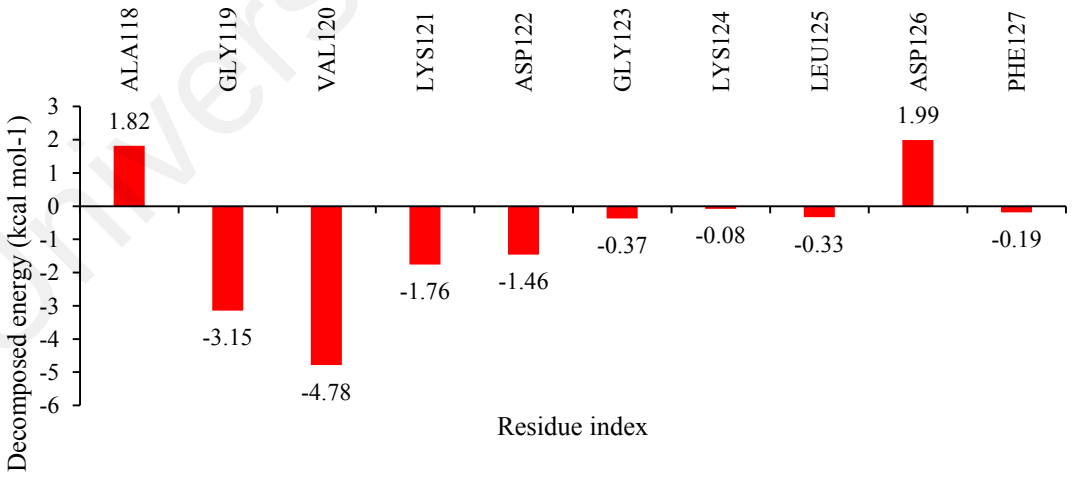

Figure 4.7: Decomposed binding free energy (kcal mol^{-1}) of DET4 on a per residue basis during 11-15 ns of the simulation time.

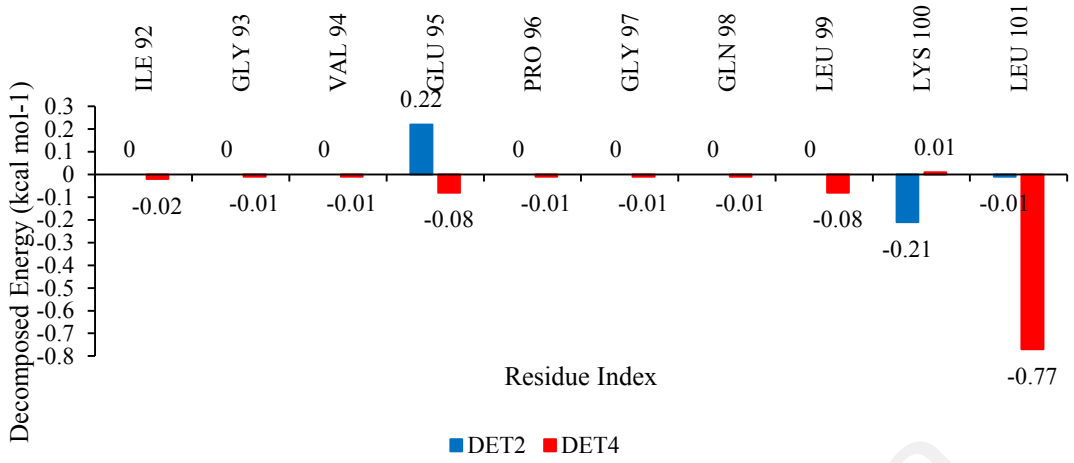

Figure 4.8: Decomposed binding free energy (kcal mol^{-1}) on the key binding site residues during 11-15 ns of the simulation time.

4.1.2.3 Hydrogen bond analysis

The hydrogen bond analysis is carried out on the trajectories from 11-15 ns. Only hydrogen bonds in agreement with the following characteristic were been taken account; i) percentage occupation greater than 50%, ii) distance of proton donor and acceptor ≤ 3.5 Å (Jeffrey, 1997) and angle of ≥ 120° for favourable hydrogen bonding (Table 4.4). DET4-bound complex forms two hydrogen bonds between GLY119 − HIS112 and VAL120 – HIS115, while none has been observed from the DET2-bound complex. Also, GLY119 and VAL120 of DET4 that showed favourable binding interactions in the decomposition analysis are found to form a hydrogen bond with the domain III binding pocket (Table 4.4). The number of hydrogen bonds between the peptides and protein alone can explain the reason why DET4 interacts with the domain III distinctively from the other peptides.

Table 4.4: Hydrogen bond formation of DET4-bound complex.

Complex	Proton acceptor	Proton donor	% occupied	Distance (Å)	Angle (°)
DET4+Domain III	GLY_119@O	HIS_112@NE2	60.60	2.85	153.48
	VAL_120@O	HIS_115@N	55.44	2.87	156.78

4.1.3 Single point mutation of DET4 residues

According to Sammond et al. (2007), the criteria of point mutations that will improve the affinity of the protein-protein interface are: 1) the mutation must be from a polar amino acid to a non-polar amino acid or from a non-polar amino acid to a larger non-polar amino acid, 2) the free energy of binding as calculated should be more favourable than the free energy of binding calculated for the wild-type complex, and 3) the mutation should not be predicted to significantly destabilize the monomers. Residues in DET4 that contribute to less favourable binding free energy identified from our previous work were mutated according to the suggestions from the BeAtMuSiC server and amino acid substitution matrix. The mutation point that predicted to increase the binding free energy is illustrated in Table 4.5.

Table 4.5: Single point mutation suggestions by BeAtMuSiC server and amino acid substitution matrix.

DET4 (residues with less favourable binding to domain III)	BeAtMuSiC server		Amino acid substitution matrix
	Amino acid	ΔΔGBind (kcal mol^{-1})	
ALA118	GLY	-0.37	SER
GLY123	TRP	-0.28	ASN
LYS124	THR	-0.13	ARG
LEU125	ASP	-0.16	ILE
ASP126	PRO	-0.22	ASN
PHE127	GLU	-0.25	TYR

4.1.4 Molecular dynamic simulations of modified peptides

4.1.4.1 Binding free energy of the DET4 and modified peptides

As stated in previous findings, the MM-PBSA approach was used to calculate the binding free energy for modified peptides. The last 5 ns trajectories of the MD simulations were selected to examine the effect of mutation by both mentioned methods (Table 4.6 and Figure 4.9). Most of the energy contributions were from the electrostatic (EEL) term rather than van der Waals (vdW) interaction. Out of twelve mutations, only six modifications were observed to have an increased binding affinity, half of which successfully increased the binding affinity by more than 9.6 kcal mol^{-1}. Mutation of

L125D and D126P from BeatMuSic prediction and L125I by amino acid substitution results in a more favourable binding free energy ($\Delta E_{binding}$) compared to that for DET4. Substituting LEU with negatively charged ASP improved the binding affinity due to having more favourable polar interactions and promoting favourable contacts with the binding site, especially for residue LYS100 which one of the binding site residues, in the case of L125I (Figure 4.10). Mutating LYS124 to THR and PHE127 to GLU based on BeatMuSic server prediction and LYS124 to ARG and ASP126 to ASN based on the amino acid substitution matrix destabilizes the complexes, probably due to unfavourable backbone and side chain conformation in the bound complexes, e.g. changing of ALA118 to relatively small and flexible GLY.

Table 4.6: MM-PBSA free energy binding prediction for 12 complexes after the single point mutation on DET4.

MM-PBSA $\Delta E_{binding}$ (kcal mol^{-1})							
DET4	A118G	G123W	K124T	L125D	D126P	F127E	BeatMuSic server
-32.60	-12.93	-36.79	-31.16	-42.85	-47.97	-21.75	
	A118S	G123N	K124R	L125I	D126N	F127Y	Amino acid substitution max
	-35.85	-32.18	-27.74	-42.24	-27.82	33.63	

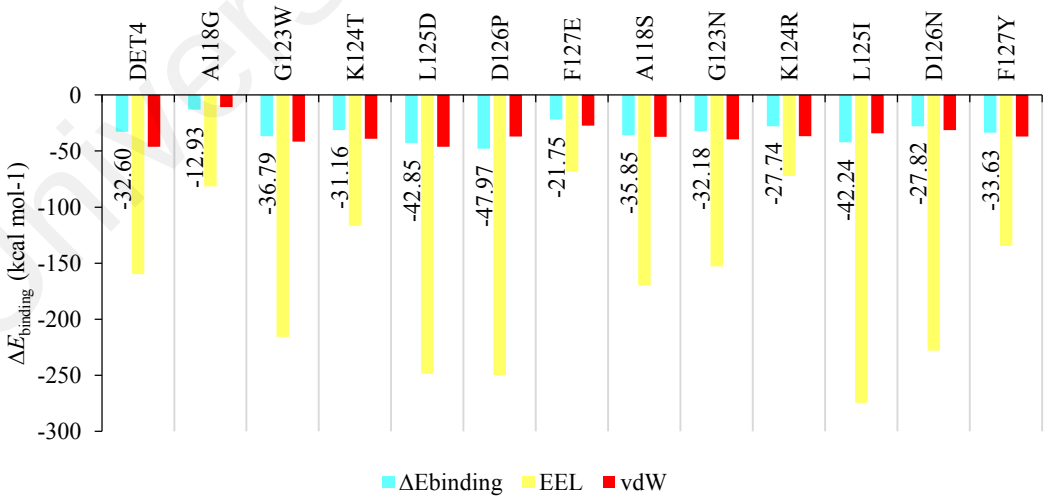

Figure 4.9: Relative binding free energies of complexes estimated using MM-PBSA. The EEL and vdW represent the electrostatic and van der Waals contributions from MM, respectively. $\Delta E_{binding}$ (in kcal mol^{-1}, binding energy neglecting the contribution of entropy) is the final estimated binding free energy calculated by MM-PBSA.

4.1.4.2 Important residues involving the binding

Mutation of L125D, L125I, and D126P at DET4 showed the best improvement among all the 12 modifications and produced better binding free energies as compared to DET4. Per residue decomposition analysis upon the binding of the improved peptide with mutations at the position of 125 and 126 revealed that from the binding site of the domain III, LEU99, LYS100 and LEU101 are strongly involved in the binding of these newly improved peptides (i.e. L125D, L125I, and D126P) **(**Figure 4.10**)**. All modified peptides show better contact with the binding pocket of the domain III compared to that of DET4. The small contribution on position 92 to 98 residues indicates that the peptides are drifted away from the pocket throughout the simulations and have shifted their contacts to the other side of the binding pocket adjacent to the postulated binding pocket **(**Figure 4.11).

Figure 4.10: Relative binding free energies on a per residues basis computed using last 5 ns trajectories of the MD simulation, for the domain III binding pocket upon the binding of the peptides.

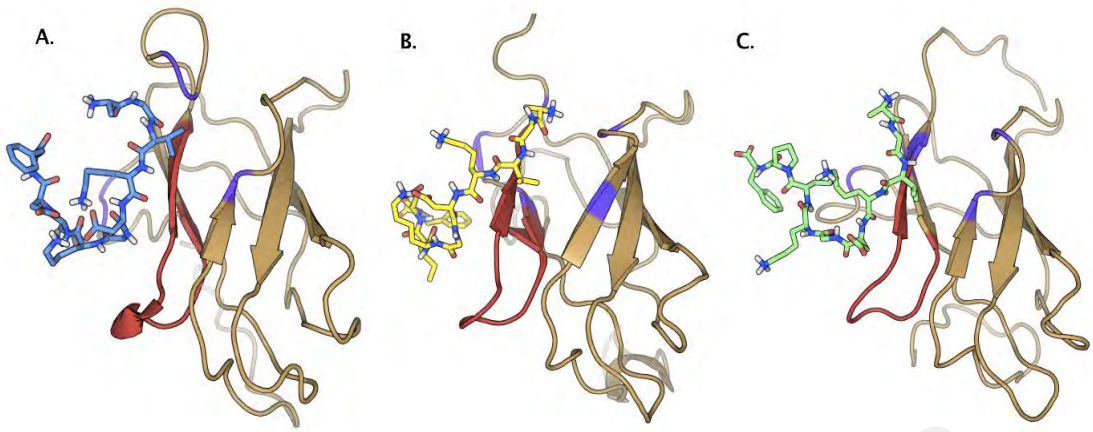

Figure 4.11: Snapshots of A. L125D, B. L125I, and C. D126P bound complexes at 10 ns MD simulations. Peptides are shown in stick representation. Only the polar hydrogen are shown. Domain III are coloured in brown, with the binding site highlighted in red. Peptides were found to make additional contacts with residues adjacent to the postulated binding pocket.

4.1.4.3 Hydrogen bond analysis of best modified peptides (L125D, D126P, and L125I)

The modified peptides of L125D, D126P, and L125I were observed to be the potential peptides that enhance the binding affinity with domain III. The analyses of the hydrogen bond formation for the last 5 ns trajectories with the following characteristics; i) percentage occupation greater than 50%, ii) distance of proton donor and acceptor ≤ 3.5 Å (Jeffrey, 1997) and angle of ≥ 120° were tabulated in Table 4.7. The peptide of L125I has four hydrogen bonds interaction, followed by D126P with two hydrogen bonds and only one was formed in the L125D complex. The L125D peptide form hydrogen bonds with LYS100 amino acid, L125I peptide was found to form favourable hydrogen bonds with LYS100, HIS115 and GLN98 and D126P peptide with LYS100 residue. The binding pocket residue, LYS100, contributed most in forming favourable binding interaction with the modified peptides, correlated to the result of decomposition energy per residue (Figure 4.10).

Table 4.7: Hydrogen bond formation of L125D, D126P and L125I simulations.

Complex	Proton acceptor	Proton donor	% occupied	Distance (Å)	Angle (°)
L125D	LYS_100@O	LYS_121@N	54.00	2.89	153.89
D126P	LYS_121@O	LYS_100@N	80.16	2.85	158.23
	LYS_100@O	LYS_121@N	74.68	2.85	157.79
L125I	LYS_121@O	LYS_100@N	79.56	2.85	159.10
	LYS_100@O	LYS_121@N	64.72	2.86	155.97
	HIS_115@O	GLY_119@N	57.24	2.85	156.10
	GLN_98@O	GLY_123@N	50.76	2.87	147.34

Note: residues from L125D, D126P and L125I are coloured red, green and purple respectively

Two modified peptides, L125D and L125I, demonstrated better binding free energy among all the 12 modifications carried out compared to the original peptide-DET4. These were further tested in *in vitro* to determine their effect on the dengue virus infectibility (Appendix A and B). The D126P peptide was excluded in this experiment because proline could probably induce disruption on the peptide stability or protein's secondary structure; Due to its cyclic residue, Proline does not have hydrogen on its α amino group which makes it unable to contribute to a hydrogen bonding interaction during peptide bond formation.

4.2 *In silico* screening for mechanism study of antidiabetic compounds

4.2.1 Binding affinity with protein targets from *in silico* molecular docking

Nojirimycin, the most renowned glucosidase inhibitors since forty years passed was first reports in 1966 (Bertozzi & Kiessling, 2001; Ishida et al., 1967). Since then, a large of number of these inhibitors have been discovered, synthesized and studied for their inhibitory activity. Some research reported α-glucosidase inhibitors to have the following characteristics: (1) sugar (substrate)-mimic structures, (2) the ability to form ionic bonds with nucleophilically catalysing residues, (3) transition-state-like structures, (4) the ability to form hydrogen bonds with catalytic acid residues, (5) the ability to make ionic and hydrophobic interactions at sites other than active sites and (6) the ability to form covalent bonds with enzyme through an epoxy or aziridine group (Hakamata et al., 2009). Thus, all the criteria of these α-glucosidase inhibitors were investigated by computational

methods with possible ligands of angustine, (E)-labda-8(17),12-diene-15,16-dial and zerumin A.

Docking studies were performed to gain insight a preferable binding conformation of ligands with the target protein. The result with rigid docking indicated that the ligands are active with the negative binding affinity range -9.8 to -6.6 kcal mol^{-1} in Table 4.8. The more negative and low value of binding affinity indicated strongly favourable bonds between receptor and peptides, indicating that peptides were in its most stable conformation. Docking study revealed the standard (acarbose), known as sugar derivatives which are in clinical use showed the lowest binding affinity compared to other ligands in α-glucosidase. However, the experimental results from our collaborator reported (E)-labda-8(17),12-diene-15,16-dial as the most active against this target protein with IC_{50} of 39.7 ± 1.09 μM. This due to the high number of hydroxyl groups in acarbose and this ligand was originally in 1AGM that makes it specific for the binding site residue (Bharatham et al., 2008). In addition, docking is a primary analysis as its results will be further validated with a more stringent computational approach such as molecular dynamic simulations.

Table 4.8: Molecular docking results with AutodockVina of ligands.

Receptor	Ligands	IC_{50}±SEM (μM)	Binding Affinity (kcal mol^{-1})
α-Glucosidase	Angustine	48.1±2.5	-9.5
	(*E*)-labda-8(17),12-diene-15,16-dial	39.7±1.09	-7.2
	Zerumin A	53.3±2.94	-6.6
	Standard (Acarbose)	840±1.73	-9.8

Note: The IC_{50} was performed by our collaborator (unpublished data).

4.2.2 Molecular dynamic simulations of ligands

4.2.2.1 Dynamics conformational changes of protein-ligand complex

Best conformation of angustine and (E)-labda-8(17),12-diene-15,16-dial and the standard, acarbose from docking were analysed by MD simulation to study the binding mechanism. While, the MD simulation was not performed to zerumin A as it showed the least activity based on the experimental supported by the docking result compared with angustine and (E)-labda-8(17),12-diene-15,16-dial. The trajectory stability was monitored and confirmed by the analysis of Root mean squared deviations (RMSD) of all Cα-atoms in Figure 4.12 as it can differentiate the quality of the structure. A high value of RMSD indicates the poor quality of protein structure (Law et al., 2005). In this study, angustine showed a good value of RMSD that demonstrates the structure was stable over the simulation time as it was oscillating steadily within a small range compared to others. RMSD of (E)-labda-8(17),12-diene-15,16-dial increased dramatically at 8ns showed the instability of structural changes during the simulation.

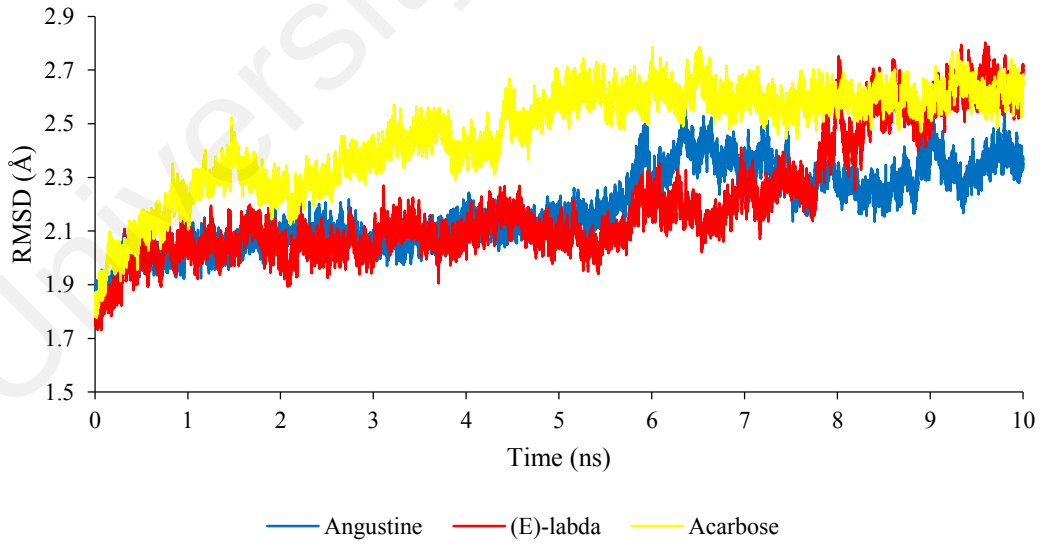

Figure 4.12: Root mean squared deviations (RMSD) of all Cα-atoms of α-glucosidase with angustine (blue), (E)-labda-8(17),12-diene-15,16-dial (red) and acarbose (yellow) along simulation time.

4.2.2.2 Binding free energy analysis

The contribution of energies and binding free energy of each complex were tabulated in Table 4.9 based on both approaches of MM-PBSA/GBSA. However, the calculations from MM-GBSA of 6 to 10 ns were approximated to the experimental value with a lower standard error of the mean whereas MM-PBSA protocol did not give any good correlations. Angustine showed a lower $\Delta E_{\text{MM-GBSA}}$ value of -23.58 kcal mol^{-1} compared to (E)-labda-8(17),12-diene-15,16-dial (-12.70 kcal mol^{-1}) and acarbose (-6.23 kcal mol^{-1}) at last 5 ns of simulation with α-glucosidase. The main contribution of energy was from van der Waal's forces rather than an electrostatic force for both angustine and (E)-labda-8(17),12-diene-15,16-dial while it was vice versa for binding of acarbose. For a protein-ligand complex, properties calculated from MM-GBSA protocol is more often reported in the literature, in which it also provides a good correlation to experimental results (Genheden and Ryde, 2015).

Table 4.9: MM-PBSA/GBSA calculation during 6-10 ns of the MD simulations for α-glucosidase and selected ligands.

Energy term	Angustine-bound complex (kcal mol^{-1})	(E)-labda-8(17),12-diene-15,16-dial-bound complex (kcal mol^{-1})	Acarbose-bound complex (kcal mol^{-1})
EEL	-5.60 ± 1.65	-3.21 ± 2.11	-66.51 ± 9.59
vdW	-38.59 ± 2.04	-21.62 ± 1.93	-24.80 ± 4.04
$\Delta G_{\text{sol (MM-PBSA)}}$	28.50 ± 3.35	17.09 ± 3.57	81.15 ± 8.61
$\Delta G_{\text{sol (MM-GBSA)}}$	20.61 ± 1.59	12.13 ± 1.85	85.09 ± 7.13
$\Delta E_{\text{MM-PBSA}}$	-15.69 ± 3.35	-7.74 ± 3.05	-10.17 ± 6.70
$\Delta E_{\text{MM-GBSA}}$	-23.58 ± 2.13	-12.70 ± 1.77	-6.23 ± 3.47

Note: The EEL and vdW represent the electrostatic and van der Waals contributions from MM, respectively. ΔGsol $_{\text{(MM-PBSA/GBSA)}}$ stands for electrostatic and nonpolar contribution to the solvation energy. $\Delta E_{\text{MM-PBSA/GBSA}}$ (in kcal mol^{-1}, binding energy neglecting the contribution of entropy) is the final estimated binding free energy calculated.

4.2.2.3 Significant residues involving the interaction of complexes

Decomposed calculated binding free energies were analysed to investigate the important amino acid residues that show strong interactions with the target protein. Figure 4.13 illustrates the results of this analysis by plotting the decomposed energies against

significant amino acid residues of each complex. The positive and negative values indicate the unfavourable and favourable contribution, respectively. Note that residue contributes to large relative energy (≥ -1.00 kcal mol^{-1}) were considered as a key amino acid residue of the complex.

Several residues of TRP50, TRP175, GLU 177, ARG301 and TYR307 were identified to have a significant contribution to the energy in angustine-bound complex with a negative energy value of -1.08, -1.37 -1.07, -2.06, and -2.98 kcal mol^{-1} respectively. While, TYR46, TRP117 and TYR307 were verified as important amino acids residue for (E)-labda-8(17),12-diene-15,16-dial-bound complex with the contribution of energy -1.50, -1.10 and -1.91 kcal mol^{-1} respectively. Acarbose-bound complex has contact with important amino acids of PRO44, ARG52, TRP117, GLU176, ARG301 and TYR307 with an energy value of -1.32, -7.03 -1.26, -1.25, -1.27 and-1.03 kcal mol^{-1} respectively. ARG52 contributed most energy contribution in the acarbose-bound complex as it forms favourable three hydrogen bonds and a single salt bridge with protein residues (Table 4.10). In addition, all ligand-bound complexes were observed to have contact with ARG52, TRP117 and TYR307 in terms of negative energy value. The favourable ligand-bound complexes interaction has also been contributed by residue involved in binding site; ARG52 and ARG301 (Aleshin et al., 1994).

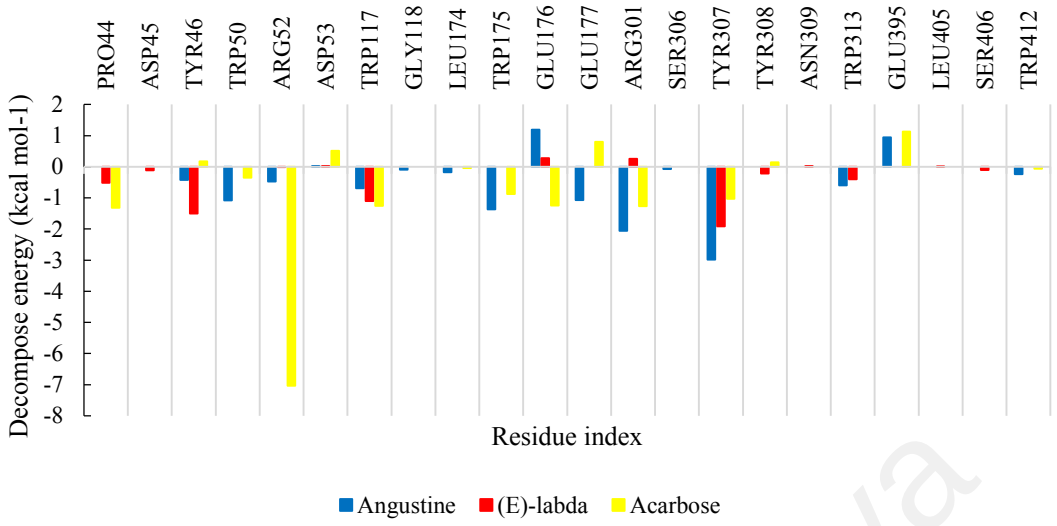

Figure 4.13: Decomposition of binding energy on a per residue within 3 Å region and binding site of α-glucosidase during 6-10 ns simulation.

The interaction of ligands-bound complexes revealed a strong contribution of important residue. Table 4.10 showed possible interaction that each of the ligands had based on analysis by Discovery Studio 4.5 visualizer and Protein-Ligand Interaction Profiler (PLIP) server. As mentioned by Hakamata et al. (2009), hydrophobic interactions were found at the angustine-bound complex where it was one of the characteristics to be potent inhibitors with the ability to make hydrophobic interactions at sites other than the binding site. TRP50, TRP117, TYR307 and TRP313 were observed to have hydrophobic interactions with other residues from active site residues. The same goes for (E)-labda-8(17),12-diene-15,16-dial-bound complex where h-bond is formed between SER406 and O1 atom of the ligand. Hydrophobic interaction was also found other than active site residue of TYR308 with a distance of 3.92 Å. In addition, acarbose had the ability to form hydrogen bonds with the catalytic acid residue of GLU176 of target protein, 1AGM. The salt bridge formation of ARG52 with the carboxylate group contributes to the stability and specificity of interaction of proteins with the ligand, acarbose (Bosshard et al., 2004). Acarbose-bound complex form six h-bonds with a distance range of 1.64 Å to 2.86 Å.

Table 4.10: Type of interaction in ligands-bound complexes.

Angustine-bound complex				
Type of interaction	Residue	Distance (Å)	Protein atom	Ligand atom
Hydrophobic	TRP50	3.25	CZ2	C20
	TRP117	3.80	CD2	C24
	TRP117	3.68	CZ2	C23
	TYR307	3.93	CE1	C5
	TYR307	3.84	CE2	C6
	TRP313	3.80	CH2	C6
(E)-labda-8(17),12-diene-15,16-dial-bound complex				
Type of interaction	Residue	Distance (Å)	Protein atom	Ligand atom
Hydrogen bond	SER406	2.15	H	O1
Hydrophobic	TYR308	3.92	CE1	C16
Acarbose-bound complex				
Type of interaction	Residue	Distance (Å)	Protein atom	Ligand atom
Hydrogen bond	ARG52	2.29	HH12	O1D
	ARG52	2.37	HH12	O2D
	ARG52	2.17	HH22	O2D
	GLU176	1.64	OE1	H43
	GLU177	2.86	OE2	H45
	GLU176	2.83	OE1	H41
Salt bridge	Arg52	4.93	CZ	OD1,OD5

As shown in Figure 4.14, ligand **a**. angustine **b**. (E)-labda-8(17),12-diene-15,16-dial and **c**. acarbose was observed with important amino acid residue that contributes negative value in 3 Å region. A close view of interactions has been depicted; whereas green dotted lines represent hydrogen bonds, the orange line represents a salt bridge and the red line represent hydrophobic. All the graphics were generated by Pymol version 1.3.

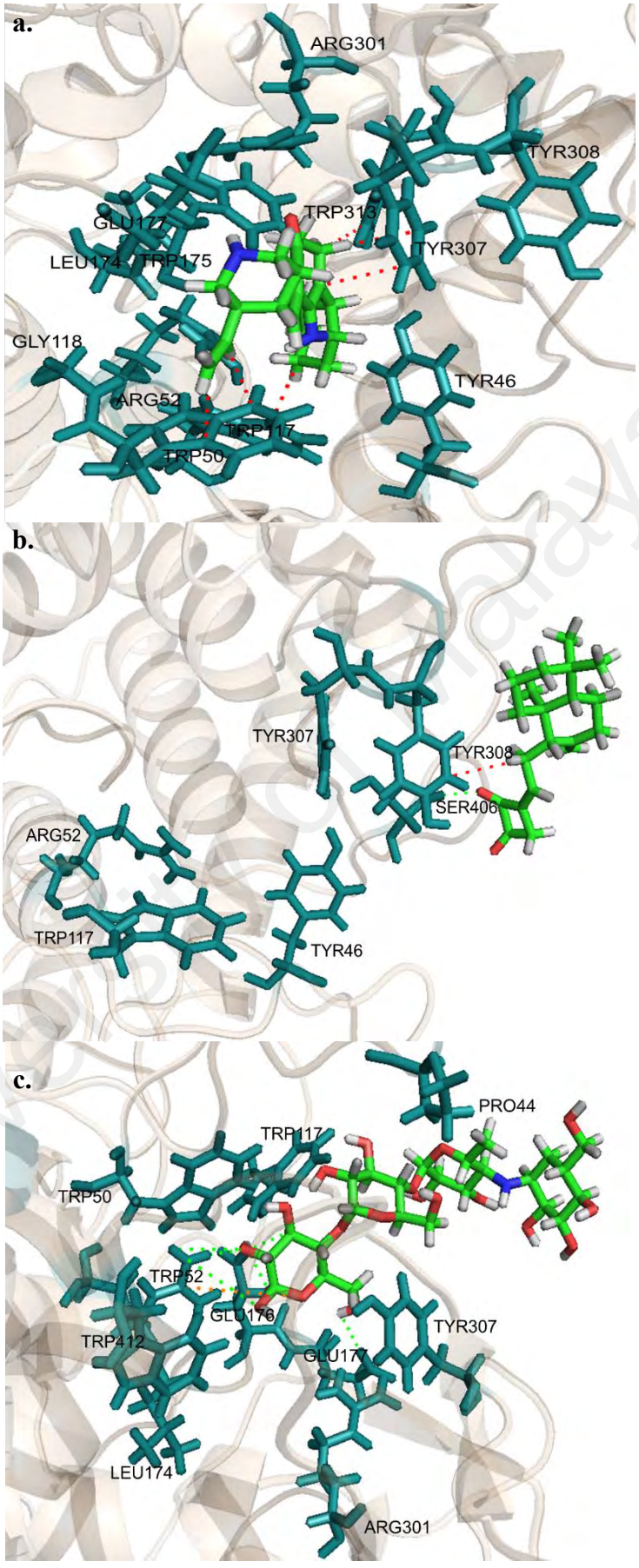

Figure 4.14: The interaction between 1AGM, α-glucosidase and the ligands, a. angustine, b. (E)-labda-8(17),12-diene-15,16-dial and c. acarbose.

CHAPTER 5: CONCLUSION AND FUTURE WORKS

5.1 Conclusion

As a conclusion, the integrated computer-assisted strategies were applied to process the huge amount of available structural and biological information in a reasonable time to study the mechanism of bioactive compounds against selected diseases. Together with the collaborative computational and experimental outcome, these integrated computational approaches offer an efficient approach to discover the potential lead compounds and their activity. The analysis of MD trajectories reveals stability, thermal motion, binding affinity and decomposition per residue of important amino acids contribute to the binding of protein-peptide and protein-ligand bound complex. MM-PBSA and MM-GBSA approaches are used in estimating the binding free energy of complexes that leads to correlation towards IC_{50} results making the computational data reliable. Thus, several improvements and continuous efforts need to be done in developing and designing more potent analogous peptides and ligands against infection, for example, dengue case study where the peptides would be tested against different strains and serotype available by computational and clinical methods.

In silico compounds with known potency of antiviral proved that DET4 had more favorable interaction than DET2 bound to the domain III. Decomposition analysis identified residue LEU 120 and PRO 122 of DET2 and residue GLY 119, VAL 120, LYS 121, and ASP 122 of DET4 as major contributors in the binding. These residues also associated with the high occupancy hydrogen bonding between the peptide and domain III. Several residues were shown to contribute less favorably to the binding; ALA 118, GLY 123, LYS 124, LEU 125, ASP 126 and PHE 127 of DET4 were further to be improved. Enhancement in the binding affinity of the single point mutated peptides of L125D, L125I, and D126P to the domain III of E glycoprotein revealed several key residues (i.e. LEU99, LYS100 and LEU101) involving in the binding pocket of domain

III. HIS115 and GLN98 also gave significant energy contribution in L125I by offering a favourable hydrogen bond interaction.

The computational approach of *in silico* compounds with known potency of antidiabetic compounds generates comparable data and results correspond to the experimental studies where angustine was reported as the most active compound for α-glucosidase of the target protein. Residues of TRP50, TRP175, GLU177, ARG301 and TYR307 were identified as a major contribution to the lowest binding energy in angustine-bound complex. ARG52 and ARG301 also were identified to have a favorable interaction in the binding pocket residue with the compounds. Thus, with the knowledge of the binding conformation between ligands and target protein obtained from the molecular docking and MD simulation, angustine could be the potential and potent drug to develop for α-glucosidase inhibitors.

5.2 Future works

Continuous effort is undergoing to develop these antiviral peptides to a novel therapeutics for dengue virus infection that active against all the serotypes (because the lateral loop is a conserved region). The antiviral peptides required more modification on less favorable residues through single point mutation and binding affinity calculation in a reasonable time scale of molecular dynamics simulation. A study across of DENV2 strain especially mutation on the binding site region should be included to test the effectiveness of these antiviral peptides in blocking the receptor attachment site on the envelope protein and subsequently stop the virus from attaching to the host and probably potential to be active against all the serotypes of dengue (because the lateral loop is a conserved region).

In the antidiabetic study, natural plants offer a promising potential as pharmaceutical agents to be developed as α-glucosidase inhibitors, which is safer and more convenient

than synthetic drugs. Therefore, the promising results shall be carried forward with prolonging the simulation time (up to 100 ns) to observe the stability and binding free energy of the complex. *In silico* ADMET could be performed before *in vivo* test to give prediction in absorption, distribution, metabolism, excretion and toxicity of compounds before further verify the activity.

REFERENCES

Accelrys. (2009). *Discovery Studio (version 2.5.5)*. San Diego, California, USA.

Adcock, S.A., & McCammon, J.A. (2006). Molecular dynamics: Survey of methods for simulating the activity of proteins. *Chemical Reviews, 106*, 15891615.

Aleshin, A.E., Firsov, L.M., & Honzatko, R.B. (1994). Refined structure for the complex of acarbose with glucoamylase from Aspergillus awamori var. X100 to 2.4-A resolution. *Journal of Biological Chemistry, 3*, 15631-15639.

Alhoot, M.A., Rathinam, A.K., Wang, S.M., Manikam, R., & Sekaran, S.D. (2013). Inhibition of dengue virus entry into target cells using synthetic antiviral peptides. *International Journal of Medical Sciences, 10*, 719-729.

American Diabetes Association. (2010). Standards of medical care in diabetes-2010. *Diabetes Care, 33*, S11-S61.

American Diabetes Association. (2011). Standards of medical care in diabetes-2011. *Diabetes Care, 34*, S11-S61.

Anam, K., Widharna, R.M., & Kusrini, D. (2009). α-glucosidase inhibitor activity of Terminalia species. *International Journal of Pharmaceutics, 5*, 277-280.

Arun, B. (2009). Challenges in drug discovery: Can we improve drug development. *Journal of Bioanalysis and Biomedicine, 1*, 50-53.

Awang, K., Ibrahim, H., Syamsir, D.S., Mohtar, M., Ali, R.M., & Ali, N.A.M. (2011). Chemical constituents and antimicrobial activity of the leaf and rhizome oils of *Alpinia pahangensis*Ridl., an endemic wild ginger from Peninsular Malaysia. *Chemistry and Biodiversity, 8*, 668-673.

Awin, T., Mediani, A., Faudzi, S.M.M., Leong, S.W., Shaari, K., & Abas, F. (2020) Identification of α-glucosidase inhibitory compounds from *Curcuma mangga* fractions. *International Journal of Food Properties, 23*, 154-166.

Azam, S.S., Uddin, R., & Wadood, A. (2012). Structure and dynamics of alpha-glucosidase through molecular dynamics simulation studies. *Journal of Molecular Liquids, 174*, 58-62.

Baharuddin, A., Amir Hassan, A., Othman, R., Xu, Y., Huang, M., Ario Tejo, B., … Othman, S. (2014). Dengue envelope domain III-peptide binding analysis via tryptophan fluorescence quenching assay. *Chemical and Pharmaceutical Bulletin (Tokyo), 62*, 947-955.

Baig, M.H., Ahmad, K., Adil, M., Khan, Z.A., Khan, M.I., Lohani, M., … Kamal, M.A. (2014). Drug discovery and *in silico* techniques: A mini-review. *Enzyme Engineering, 4*, 1-3.

Bayly, C.I., Cieplak, P., Cornell, W., & Kollman, P.A. (1993). A well-behaved electrostatic potential based method using charge restraints for deriving atomic charges: the RESP model. *The Journal of Physical Chemistry, 97*, 10269-10280.

Bertozzi, C.R., & Kiessling, L.L. (2001). Chemical glycobiology. *Science, 291*, 2357-2364.

Bharath, E.N., Manjula, S.N., & Vijaychand, A. (2011). *In silico* drug design- tool for overcoming the innovation deficit in the drug discovery process. *International Journal of Pharmacy and Pharmaceutical Sciences, 3*, 8-12.

Bharatham, K., Bharatham, N., Park, K.H., & Lee, K.W. (2008). Binding mode analyses and pharmacophore model development for sulfonamide chalcone derivatives, a new class of α-glucosidase inhibitors. *Journal of Molecular Graphics and Modelling, 26*, 1202-1212.

Bhatt, S., Gething, P.W., Brady, O.J., Messina, J.P., Farlow, A.W., Moyes, C.L., … Hay, S.I. (2013). The global distribution and burden of dengue. *Nature, 496*, 504-507.

Bischoff, H. (1995). The mechanism of alpha-glucosidase inhibition in the management of diabetes. *Clinical and Investigative Medicine, 18*, 303-311.

Blake, R.A. (2007). Target validation in drug discovery. *Method Molecular Biology, 356*, 367-377.

Bordo, D., & Argos, P. (1991). Suggestions for "safe" residue substitutions in site-directed mutagenesis. *Journal of Molecular Biology 217*, 721-729.

Bosshard, H.R., Marti, D.N., & Jelesarov, I. (2004). Protein stabilization by salt bridges: Concepts, experimental approaches and clarification of some misunderstandings. *Journal of Molecular Recognition, 17*, 1-16.

Boulton, A.J., Vinik, A.I., Arezzo, J.C., Bril, V., Feldman, E.L., Freeman, R., … Ziegler, D. (2005). Diabetic neuropathies: A statement by the American Diabetes Association. *Diabetes Care 2005, 28*, 956-962.

Brady, O.J., Gething, P.W., Bhatt, S., Messina, J.P., Brownstein, J.S., Hoen, A.G., … Hay, S.I. (2012). Refining the global spatial limits of dengue virus transmission by evidence-based consensus. *PLoS Neglected Tropical Disease, 6*, Article#e1760.

Bray, G.A., & Greenway, F.L. (1999). Current and potential drugs for treatment of obesity. *Endocrine Reviews, 20*, 805–875.

Bressanelli, S., Stiasny, K., Allison, S.L., Stura, E.A., Duquerroy, S., Lescar, J., … Rey, F. (2004). Structure of a flavivirus envelope glycoprotein in its low-pH-induced membrane fusion conformation. *EMBO Journal, 23*, 728-738.

Brooks, B.R., Bruccoleri, R.E., Olafson, B.D., States, D.J., Swaminathan, S., & Karplus, M. (1983) CHARMM - A programme for macromolecular energy, minimization, and dynamics calculations. *Journal of Computational Chemistry, 4*, 187-217.

Bulobangkal. (2019). *StuartXchange*. Retrieved on February 5, 2020 from http://www.stuartxchange.org/index.html.

Burn, E.N., Taiwe, G.S., Moto, F.C.O., Ngoupaye, G.T., Nkantchoua, G.C.N., Pelanken, M.M., … Rakotonirina, A. (2009). Anticonvulsant, anxioloytic, and sedative properties of the roots of *Nauclea latifolia* Smith in mice. *Epilepsy and Behavior, 15*, 434-440.

Buysschaert, M., Dramaix, A.S., Wallemacq, P., & Hermans, M. (2000). Hyperhomocysteinemia in type 2 diabetes: Relationship to macro angiopathy, nephropathy and insulin resistance. *Diabetes care, 23*, 1816-1822.

Case, D.A., Darden, T.A., Cheatham, TEIII., Simmerling, C.L., Wang, J., Duke, R.E., … Kollman, P.A. (2012). AMBER 12. University of California, San Francisco.

Champagne, K., Shishido, A., & Root, M.J. (2009). Interactions of HIV-1 inhibitory peptide T20 with the gp41 N-HR coiled coil. *Journal of Biological Chemistry, 284*, 3619-3627.

Chan, D.C., & Kim, P.S. (1998). HIV entry and its inhibition. *Cell, 93*, 681-684.

Chang, M.W, Ayeni, C., Breuer, S., & Torbett, B.E. (2010). Virtual screening for HIV protease inhibitors: A comparison of AutoDock 4 and Vina. *PLoS ONE, 5*, Article#e11955.

Chen, Y., Maguire, T., Hileman, R.E., Fromm, J.R., Esko, J.D., Linhardt, R.J., & Marks, R.M. (1997). Dengue virus infectivity depends on envelope protein binding to target cell heparan sulfate. *Nature Medicine, 3*, 866-871.

Chiba, S. (1997). Molecular mechanism in alpha-glucosidase and glucoamylase. *Bioscience, Biotechnology, and Biochemistry, 61*, 1233-1239.

Chiu, M.W., & Yang, Y.L. (2003). Blocking the dengue virus 2 infections on BHK-21 cells with purified recombinant dengue virus 2 E protein expressed in *Escherichia coli*. *Biochemical and Biophysical Research Communications, 309*, 672-678.

Chong, L.T., Duan, Y., Wang, L., Massova, I., & Kollman, P.A. (1999). Molecular dynamics and free-energy calculations applied to affinity maturation in antibody 48G7. *Proceedings of the National Academy of Sciences of the United States of America, 96*, 14330-14335.

Clum, S., Ebner, K., & Padmanabhan, R. (1997). Cotranslational membrane insertion of the serine proteinase precursor NS2B-NS3 (Pro) of dengue virus. *Journal of Biological Chemistry, 272*, 30715-30723.

Cornell, W.D., Cieplak, P., Bayly, C.I., Gould, I.R., Merz, K.M., Ferguson, D.M., … Kollman, P.A. (1995). A second generation force eld for the simulation of proteins, nucleic acids, and organic molecules. *Journal of the American Chemical Society, 117*, 5179-5197.

Costin, J.M., Jenwitheesuk, E., Lok, S-M., Hunsperger, E., Conrads, K.A., Fontaine, K.A., … Michael, S.F. (2010). Structural optimization and de novo design of dengue virus entry inhibitory peptides. *PLoS Neglected Tropical Diseases, 4*, e721.

Crill, W.D., & Roehrig, J.T. (2001). Monoclonal antibodies that bind to domain III of dengue virus E glycoprotein are the most efficient blockers of virus adsorption to Vero cells. *Journal of Virology, 75*, 7769-7773.

Darden, T., York, D., & Pedersen, L. (1993). Particle mesh Ewald: An N log (N) method for Ewald sums in large systems. *Journal of Chemical Physics, 98*, 10089-10092.

Deen, J.L., Harris, E., Wills, B., Balmaseda, A., Hammond, S.N., Rocha, C., … Farrar, J.J. (2006). The WHO dengue classification and case definitions: Time for a reassessment. *Lancet, 368*, 170-173.

Dehouck, Y., Kwasigroch, J.M., Rooman, M., & Gilis, D. (2013). BeAtMuSiC: Prediction of changes in protein-protein binding affinity on mutations. *Nucleic Acids Research, 41*, 333-339.

Diabetes Medicines You Don't Inject. (2005). *WebMD*. Retrieved on February 5, 2020 from https://www.webmd.com/diabetes/oral-medicine-pills-treat-diabetes#1.

Dias, D.A., Urban, S., & Roessner, U. (2012). A historical overview of natural products in drug discovery. *Metabolites, 2*, 303–336.

DiMasi, J.A., Grabowski, H.G., & Hansen, R.W. (2016). Innovation in the pharmaceutical industry: New estimates of R&D costs. *Journal of Health Economics, 47*, 20-33.

Durrant, J.D., & McCammon, J.A. (2011). HBonanza: A computer algorithm for molecular dynamics trajectory hydrogen bond analysis. *Journal of Molecular Grahphics and Modelling, 31*, 5-9.

Eldridge, M.D., Murray, C.W., Auton, T.R., Paolini, G.V., & Mee, R.P. (1997). Empirical scoring functions: I. The development of a fast empirical scoring function to estimate the binding affinity of ligands in receptor complexes. *Journal of Computer-Aided Molecular Design, 11*, 425-445.

Elya, B., Basah, K., Mun'im, A., Yuliastuti, W., Bangun, A., & Septiana, E.K. (2011). Screening of α-glucosidase inhibitory activity from some plants of apocynaceae, clusiaceae, euphorbiaceae, and rubiaceae. *Natural Products for Medicine, 2012*, 1-6.

Essmann, U., Perera, L., & Berkowitz, M.L. (1995). A smooth particle mesh Ewald potential. *Journal of Chemical Physics, 103*, 8577-8593.

Ezuruike, U.F., & Prieto, J.M. (2014). The use of plants in the traditional management of diabetes in Nigeria: Pharmacological and toxicological considerations. *Journal of Ethnopharmacology, 55*, 857-924.

Falgout, B., Pethel, M., Zhang, Y.M., & Lai, C.J. (1991). Both nonstructural proteins NS2B and NS3 are required for the proteolytic processing of dengue virus nonstructural proteins. *Journal of Virology, 65*, 2467-2475.

Falgout, B., Miller, R.H., & Lai, C.J. (1993). Deletion analysis of dengue virus type 4 nonstructural protein NS2B: Identification of a domain required for NS2B-NS3 protease activity. *Journal of Virology, 67*, 2034-2042.

Fischer, P.B., Karlsson, G.B., Dwek, R.A., & Platt, F.M. (1996). N-Butyldeoxynojirimycin mediated inhibition of human immunodeficiency virus entry correlates with impaired gp120 Shedding and gp41 exposure. *Journal of Virology, 70*, 7153-7160.

Frisch M.J., Trucks, G.W., Schlegel, H.B., Scuseria, G.E., Robb, M.A., Cheeseman, J.R., … Fox, D.J. (2016). Gaussian 09, Revision A.02. Gaussian, Inc., Wallingford CT.

Gabaldón, T. (2007). Evolution of proteins and proteomes: A phylogenetics approach. *Evolutionary Bioinformatics Online, 1*, 51-61.

Gangrade, D., Sawant, G., & Mehta, A. (2016). Re-thinking drug discovery: *In silico* method. *Journal of Chemical and Pharmaceutical Research, 8*, 1092-1099.

Gaynes, R. (2017). The discovery of penicillin- new insights after more than 75 years of clinical use. *Emerging Infectious Diseases, 23*, 849-853.

Gehlhaar, D.K., Verkhivker, G.M., Rejto, P.A., Sherman, C.J., Fogel, D.B., Fogel, L.J., & Freer, S.T. (1995). Molecular recognition of the inhibitor AG-1343 by HIV-1 protease: Conformationally flexible docking by evolutionary programming. *Chemistry and Biology, 2*, 317-324.

Genheden, S., & Ryde, U. (2015). The MM/PBSA and MM/GBSA methods to estimate ligand-binding affinities. *Expert Opinion on Drug Discovery, 10*, 449-461.

Ghosh, S., & Rangan, L. (2013). *Alpinia*: The gold mine of future therapeutics. *3 Biotech, 3*, 173–185.

Götz, A.W., Williamson, M.J., Xu, D., Poole, D., Grand, S.L., & Walker, R.C. (2012). Routine microsecond molecular dynamics simulations with AMBER - Part I: Generalized born. *Journal of Chemical Theory and Computation, 8,* 1542-1555.

Grand, S.L., Götz, A.W., & Walker, R.C. (2013). SPFP: Speed without compromise - A mixed precision model for GPU accelerated molecular dynamics simulations. *Computer Physics Communications, 184*, 374-380.

Guardia, C.D. La., & Lleonart, R. (2014). Progress in the identification of dengue virus entry / fusion inhibitors. *BioMed Research International, 2014*, 1-13.

Gubler, D. J. (1998). Dengue and dengue hemorrhagic fever. *Clinical Microbiology Reviews, 11*, 480-496.

Gupta, P.P. (2014). Computer aided drug design and discovery- An economical approach to drug discovery industry. *Austin Journal of Biotechnology and Bioengineering, 1*, 2.

Guy, B., Guirakhoo, F., Barban, V., Higgs, S., Monath, T.P., & Lang, J. (2010). Preclinical and clinical development of YFV 17D-based chimeric vaccines against dengue, West Nile and Japanese encephalitis viruses. *Vaccine, 28*, 632-649.

Habibi, Z., Eftekhar, F., Samiee, K., & Rustaiyan, A. (2000). Structure and antibacterial activity of a new labdane diterpenoids from *Salvia leriaefolia*. *Journal of Natural Products, 63*, 270–271.

Hakamata, W., Kurihara, M., Okuda, H., Nishio, T., & Oku, T. (2009). Design and screening strategies for α-glucosidase inhibitors based on enzymological information. *Current Topics in Medicinal Chemistry, 9*, 3-12.

Halstead, S.B. (1988). Pathogenesis of dengue: Challenges to molecular biology. *Science, 239*, 476-481.

Halverson, J.D., Brandes, T., Lenz, O., Arnold, A., Bevc, S., Starchenko, V., … Reith, D. (2012). ESPResSo++: A modern multiscale simulation package for soft matter systems. *Computer Physics Communications, 184*, 1129-1149.

Hancock, R.E.W., & Lehrer, R. (1998). Cationic peptides: A new source of antibiotics. *Trends in Biotechnology, 16*, 82-88.

Harrison, S.C. (2008). Viral membrane fusion. *Nature Structural and Molecular Biology, 15*, 690-698.

Hotta, H., Sanchez, L.F., Takada, H., Homma, M., & Kotani, S. (1985). Enhancement of dengue virus infection in cultured mouse macrophages by lipophilic derivatives of muramyl peptides. *Microbiology and Immunology, 29*, 533-541.

Howard, C.R. (2005). *Viral hemorrhagic fever*. 1st edition, Elsevier Inc., San Diego, CA.

Hrobowski, Y.M., Garry, R.F., & Michael, S.F. (2005). Peptide inhibitors of dengue virus and West Nile virus infectivity. *Virology Journal, 2*, 49.

Hung, J.J., Hsieh, M.T., Young, M.J., Kao, C.L., King, C.C., & Chang, W. (2004). An external loop region of domain III of dengue virus type 2 envelope protein is involved in serotype-specific binding to mosquito but not mammalian cells. *Journal of Virology, 78*, 378-88.

Hussain, A., & Verma, C.K. (2017). Molecular docking and *in silico* ADMET study reveals 3-(5-{[4-(aminomethyl) piperidin-1-yl] methyl}-1h-indol-2-yl)-1h-indazole-6-carbonitrile as a potential inhibitor of cancer Osaka thyroid kinase. *Biomedical Research, 28*, 5805-5815.

Ishida, N., Kumagai, K., Niida, T., Tsuroka, T., & Yumoto, H. (1967). Nojirimycin, a new antibiotic. II. Isolation, characterization and biological activity. *Journal of Antibiotics, 20*, 66-71.

Jamaluddin, F.R., Hua, L.S., Ashaari, Z., Wahab, R., & Mohd Daud, J. (2015). Antimicrobial activities of stembark and wood extracts from *Nauclea subdita* against pathogenic microorganisms. *Malaysian Journal of Microbiology, 11*, 365-372.

Jeffrey, G.A. (1997). *An introduction to hydrogen bonding*. New York, Oxford University Press.

Jones, G., Willett, P., & Glen, R.C. (1995). Molecular recognition of receptor sites using a genetic algorithm with a description of desolvation. *Journal of Molecular Biology, 245*, 43-53.

Jones, G., Willett, P., Glen, R.C., Leach, A.R., & Taylor, R. (1997). Development and validation of a genetic algorithm for flexible docking. *Journal of Molecular Biology, 267*, 727-748.

Jorgensen, W.L., & Tirado-Rives, J. (1988). The OPLS (optimized potentials for liquid simulations) potential functions for proteins, energy minimizations for crystals of cyclic peptides and crambin. *Journal of the American Chemical Society, 110*, 1657-1666.

Kaku, K. (2010). Pathophysiology of type 2 diabetes and its treatment policy. *The Japan Medical Association Journal, 53*, 41-46.

Kaur, H., Garg, A., & Raghava, G.P.S. (2007). PEPstr: A de novo method for tertiary structure prediction of small bioactive peptides. *Protein and Peptide Letters, 14*, 626-631.

Khan, A.U., Baig, M.H., & Wadhwa, G. (2011). Molecular docking analysis of new generation cephalosporins interactions with recently known SHV-variants. *Bioinformation, 5*, 331-335.

Khan, M.S., Baig. M.H., Ahmad, S., Siddiqui, S.A., Srivastava, A.K., Srinivasan, K.V., & Ansari, I.A. (2013). Design, synthesis, evaluation and thermodynamics of 1-substituted pyridylimidazo [1,5-a] pyridine derivatives as cysteine protease inhibitors. *PloS ONE, 8*, AArticle#e69982.

Kilby, J.M., Hopkins, S., Venetta, T.M., DiMassimo, B., Cloud, G.A., Lee, J.Y., … Saag, M.S. (1998). Potent suppression of HIV-1 replication in humans by T-20, a peptide inhibitor of gp41-mediated virus entry. *Journal of Natural Medicines, 4*, 1302-1307.

Kirana, C., Record, I.R., McInthosh, G.H., & Jones, G.P. (2003). Screening for antitumor activity of 11 species of Indonesian Zingiberaceae using human MCF-7 and HT-29 cancer cells. *Pharmaceutical Biology, 41*, 271-276.

Kodchakorn, K., Dokmaisrijan, S., Chong, W.L., Payaka, A., Wisitponchai, T., Nimmanpipug, P., … Lee, V.S. (2014). GPU accelerated molecular dynamics simulations for protein-protein interaction of ankyrin complex. *Integrated Ferroelectrics, 156*, 137-146.

Kollman, P.A., Massova, I., Reyes, C., Kuhn, B., Huo, S., Chong, L., … Cheatham, T.E. (2000). Calculating structures and free energies of complex molecules:

Combining molecular mechanics and continuum models. *Accounts of Chemical Research, 33*, 889-897.

Kongsted, J., Söderhjelm, P., & Ryde, U. (2009). How accurate are continuum solvation models for drug-like molecules?. *Journal of Computer-Aided Molecular Design, 23*, 395-409.

Kramer, B., Rarey, M., & Lengauer, T. (1999). Evaluation of the FlexX incremental construction algorithm for protein-ligand docking. *Proteins, 37*, 228-241.

Król, M., Roterman, I., & Spólnik, P. (2005). Analysis of correlated domain motions in IgG light chain reveals possible mechanisms of immunological signal transduction. *Proteins, 59*, 545-554.

Kyle, J.L., & Harris, E. (2008). Global spread and persistence of dengue. *Annual Review of Microbiology, 62*, 71-92.

Lalezari, J.P., Henry, K., O'Hearn, M., Montaner, J.S., Piliero, P.J., Trottier, B., … Salgo, M. (2003). Enfuvirtide, an HIV-1 fusion inhibitor, for drug-resistant HIV infection in North and South America. *New England Journal of Medicine, 348*, 2175-2185.

Law, R.J., Capener, C., Baaden, M., Bond, P.J, Campbell, J., Patargias, G., … Sansom, M.S. (2005). Membrane protein structure quality in molecular dynamics simulation. *Journal of Molecular Graphics and Modelling, 24*, 157-165.

Leitmeyer, K.C., Vaughn, D.W., Watts, D.M., Salas, R., Chacon, I.V.D., Ramos, C., & Rico-Hesse, R. (1999). Dengue virus structural differences that correlate with pathogenesis. *Journal of Virology, 89*, 4738-4747.

Ley, S.H., Schulze, M.B., Hivert, M-F., Meigs, J.B., & Hu, F.B. (2015). Risk factors for type 2 diabetes. *Diabetes in America.* Retrieved on February 5, 2020 from https://www.niddk.nih.gov/about-niddk/strategic-plans-reports/diabetes-in-america-3rd-edition.

Liew, S.Y., Mukhtar, M.R., Abdul Hadi, A.H., Awang, K., Mustafa, M.R., Zaima, K., … Litaudon, M. (2012). Naucline, a New Indole Alkaloid from the Bark of *Nauclea officinalis*. *Molecules, 17*, 4028-4036.

Lindenbach, B.D., Thiel, H.J., & Rice, C.M. (2007). Flaviviridae: The viruses and their replication. *Fields virology,* (5th ed.), Lippincot William and Wilkins, Philadelphia.

Lok, S.M., Costin, J.M., Hrobowski, Y.M., Hoffmann, A.R., Rowe, D.K., Kukkaro, P., … Michael, S.F. (2012). Release of dengue virus genome induced by a peptide inhibitor. *PLoS One, 7*, Article#e50995.

Lopez-Rodriguez, M.L., Morcillo, M.J., Benhamu, B., & Rosado, M.L. (1997). Comparative receptor mapping of serotoninergic 5-HT3 and 5-HT4 binding sites. *Journal of Computer-Aided Molecular Design, 11*, 589-599.

MacKerell, A.D., Bashford, D., Bellott, M., Dunbrack, R.L., Evanseck, J.D., Field, M.J., … Karplus, M. (1998). All atom empirical potential for molecular modelling and dynamics studies of proteins. *Journal of Physical Chemistry, 102*, 3586-3616.

Malaysia has 3.6 million diabetics, says Dzulkefly. (2019). *The Star*. Retrieved on February 1, 2020 from https://www.thestar.com.my/news/nation/2019/03/27/ malaysia-has-36-million-diabeticssays-dzulkefly.

Malek, S.N.A., Lee, G.S., Hong, S.L., Yaacob. H., Wahab, N.A., Weber, J-F.F., & Shah, S.A.A. (2011). Phytochemical and cytotoxic investigations of *Curcuma* mangga rhizomes. *Molecules, 16*, 4539-4548.

Manaharan, T., Palanisamy, U.D., & Ming, C.H. (2012). Tropical plant extracts as potential antihyperglycemic agents. *Molecules, 17*: 5915-5923.

Mazumder, R., Hu, Z.Z., Vinayaka, C.R., Sagripanti, J.L., Frost, S.D.W., Kosakovsky Pond, S.L. & Wu, C.H. (2007). Computational analysis and identification of amino acid sites in dengue E proteins relevant to development of diagnostics and vaccines. *Virus Genes, 35*, 175-186.

Mehta, A., Zitzmann, N., Rudd, P.M., Block, T.M., & Dwek, R.A. (1998). Alpha-glucosidase inhibitors as potential broad based anti-viral agents. *FEBS Letters, 430*, 17-22.

Merad, M., Soufi, W., Ghalem, S., Boukli, F., Baig, M.H., Ahmad, K., & Kamal, M.A. (2014). Molecular interaction of acetylcholinesterase with carnosic acid derivatives: A neuroinformatics study. *CNS and Neurological Disorders Drug Targets, 13*, 440-446.

Mishra, A., Rahman, S.Z., & Khan, R.A. (2017) History of opioid addition and steps taken for de-addition. *Antrhropological Bulletin, 9*, 27-37.

Modis, Y., Ogata, S., Clements, D., & Harrison, S.C. (2004). Structure of the dengue virus envelope protein after membrane fusion. *Nature, 427*, 313-319.

Modis, Y., Ogata, S., Clements, D., & Harisson, S.C. (2005). Variable surface epitopes in the crystal structure of dengue virus type 3 envelope glycoprotein. *Journal of Virology, 79*, 1223-1231.

Mohd Bukhari, D.A., Siddiqui, M.J., Shamsudin, S.H., Rahman, M.M., & So'ad, S.Z.M. (2017). α-glucosidase inhibitory activity of selected malaysian plants. *Journal of Pharmacy and Bioallied Sciences, 9*, 164-170.

Momany, F.A., & Rone, R. (1992). Validation of the general purpose QUANTA 3.2/CHARMm force field. *Journal of Computational Chemistry*, *13*, 888-900.

Monika, G., Punam, G., Sarbjet, S., & Gupta, G.D. (2010). An overview on molecular docking. *International Journal of Drug Development and Research, 2*, 219-231.

Morris, G.M., Goodsell, D.S., Halliday, R.S., Huey, R., Hart, W.E., Belew, R.K., & Olson, A.J. (1998). Automated docking using a Lamarckian genetic algorithm and an empirical binding free energy function. *Journal of Computational Chemistry, 19*, 1639-1662.

Morris, G.M., Huey, R., Lindstrom, W., Sanner, M.F., Belew, R.K., Goodsell, D.S., & Olson. A.J. (2009). AutoDock4 and AutoDockTools4: Automated docking with selective receptor flexibility. *Journal of Computational Chemistry, 30*, 2785-2791.

Muegge, I., & Martin, Y.C. (1999). A general and fast scoring function for protein–ligand interactions: A simplified potential approach. *Journal of Medicinal Chemistry, 42*, 791-804.

Muegge, I. (2000). A knowledge-based scoring function for protein–ligand interactions: Probing the reference state. *Perspectives in Drug Discovery and Design, 20*, 99-114.

Muegge, I. (2001). Effect of ligand volume correction on PMF scoring. *Journal of Computational Chemistry, 22*, 418-425.

Mustafa, L.C.M.S., Rasotgi, C.V., Jain, C.S., & Gupta, L.C.V. (2015). Discovery of fifth serotype of dengue virus (DENV-5): A new public health dilemma in dengue control. *Medical Journal Armed Forces India, 71*, 67-70.

Nauclea subdita (Korth.) Steud. (2019). *Catalog of Life*. Retrieved on February 5, 2020 from https://www.gbif.org/species/143047562.

Nilsson, L., & Karplus, M. (1986). Empirical energy functions for energy minimization and dynamics of nucleic acids. *Journal of Computational Chemistry,* 7, 591-616.

Norrby, S. R., & Jonsson, M. (1983). Antibacterial activity of norfloxacin. *Antimicrobial Agents and Chemotherapy*, *23*, 15-18.

Ooms, F. (2000). Molecular modelling and computer aided drug design. Examples of their applications in medicinal chemistry. *Current Medicinal Chemistry, 7*, 141-158.

Oostenbrink, C., Villa, A., Mark, A.E., & van Gunsteren, W.F. (2004). A biomolecular force field based on the free enthalpy of hydration and solvation: The gromos force- field parameter sets 53A5 and 53A6. *Journal of Computational Chemistry, 25*, 1656-1676.

Otvos, L., & Wade, J.D. (2014). Current challenges in peptide-based drug discovery. *Frontiers in Chemistry, 2*, 62.

Panigrahi, S.K., & Verma, J. (2014). *Computational chemistry*. Aurigene. Bangalore, India.

Panya, A., Sawasdee, N., Junking, M., Srisawat, C., Choowongkomon, K., & Yenchitsomanus, P.T. (2015). A peptide inhibitor derived from the conserved ectodomain region of DENV membrane (M) protein with activity against dengue virus infection. *Chemical Biology and Drug Design, 86*, 1093-1104.

Parikesit, A.A., Kinanty, & Tambunan, U.S.F. (2013). Screening of commercial cyclic peptides as inhibitor envelope protein dengue virus (DENV) through molecular docking and molecular dynamics. *Pakistan Journal of Biological Sciences, 16*, 1836-1848.

Perez, A., MacCallum, J.L., Simmerling, E.B.C., & Dill, K.A. (2015). Grid-based backbone correction to the ff12SB protein force field for implicit-solvent simulations. *Journal of Chemical Theory and Computation*, *11*, 4770-4779.

Phang, C., Malek, S.N.A., & Ibrahim, H. (2013). Antioxidant potential, cytotoxic activity and total phenolic content of *Alpinia pahangensis* rhizomes. *BMC Complementary Medicine and Therapies, 13*, 1-9.

Pierson, T.C., & Diamond, M.S. (2008). Molecular mechanisms of antibody-mediated neutralisation of flavivirus infection. *Expert Reviews in Molecular Medicine, 10*, Article#e12.

Prusis, P., Junaid, M., Petrovska, R., Yahorava, S., Yahorau, A., Katzenmeier, G., …Wikberg, J.E.S. (2013). Design and evaluation of substrate-based octapeptide and non substrate-based tetrapeptide inhibitors of dengue virus NS2B–NS3 proteases. *Biochemical and Biophysical Research Communications, 434*, 767-772.

Quiroga, R., & Villarreal, M.A. (2016). Vinardo: A scoring function based on AutoDock Vina improves scoring, docking, and virtual screening. *PLoS ONE, 11*, 1-18.

Ramalho, T.C., Franca, T.C.C., Cortopassi, W.A., Goncalves, A.S., da silva, A.W.S., & da Cunha, E.F.F. (2011). Topology and dynamics of the interaction between 5-nitroimidazole radiosensitizers and duplex DNA studied by a combination of docking, molecular dynamic simulations and NMR spectroscopy. *Journal of Molecular Structure, 992*, 65-71.

Rarey, M., Kramer, B., Lengauer, T., & Klebe, G. (1996). A fast flexible docking method using an incremental construction algorithm. *Journal of Molecular Biology, 261*, 470-489.

Rey, F.A., Heinz, F.X., Mandl, C., Kunz, C., & Harrison, S.C. (1995). The envelope glycoprotein from tick-borne encephalitis virus at 2 Å resolution. *Nature, 375*, 291-298.

Richomme, P., Godet, M. C., Foussard, F., Toupet, L., Sevenet, T., & Bruneton, J. (1991). A novel leishmanicidal labdane from Polyalthia macropoda. *Planta Medica, 57*, 552–554.

Röckendorf, N., Borschbach, M., & Frey, A. (2012). Molecular evolution of peptide ligands with custom-tailored characteristics for targeting of glycostructures. *PLoS Computational Biology, 8*, 1-10.

Roe, D.R., & Cheatham, T.E. (2013). PTRAJ and CPPTRAJ: Software for processing and analysis of molecular dynamics trajectory data. *Journal of Chemical Theory and Computation, 9*, 3084-3095.

Salomon-Ferrer, R., Götz, A.W., Poole, D., Grand, S.L., & Walker, R.C. (2013). Routine microsecond molecular dynamics simulations with AMBER on GPUs. 2. Explicit solvent particle mesh Ewald. *Journal of Chemical Theory and Computation, 9*, 3878-3888.

Sammond, D.W., Eletr, Z.M., Purbeck, C., Kimple, R.J., Siderovski, D.P., & Kuhlman, B. (2007). Structure-based protocol for identifying mutations that enhance protein-protein affinities. *Journal of Molecular Biology, 371*, 1392-1404.

Sampath, A., & Padmanabhan, R. (2009). Molecular targets for flavivirus drug discovery. *Antiviral Research, 81*, 6-15.

Schmidt, A.G., Yang, P.L., & Harrison, S.C. (2010a). Peptide inhibitors of flavivirus entry derived from the E protein stem. *Journal of Virology, 84*, 12549-12554.

Schmidt, A.G., Yang, P.L., & Harrison, S.C. (2010b). Peptide inhibitors of dengue-virus entry target a late-stage fusion intermediate. *PLoS Pathoens., 6*, e1000851.

Schrödinger. (2015). *The PyMOL Molecular Graphics System (Version 1.6)*. New York, USA.

Seema, & Jain, S.K. (2005). Molecular mechanism of pathogenesis of dengue virus: Entry and fusion with target cell. *Indian Journal of Clinical Biochemistry, 20*, 92-103.

Shan, Y., Kim, E.T., Eastwood, M.P., Dror, R.O., Seeliger, M.A., & Shaw, D.E. (2011). How does a drug molecule find its target binding site?. *Journal of the American Chemical Society, 133*, 9181-9183.

Sheeja, A.D.B., & Nair, M.S. (2014). Facile isolation of (E)-labda-8(17),12-diene-15,16-dial from *Curcuma amada* and its conversion to other biologically active compounds. *Indian Journal of Chemistry, 53B*, 319-324.

Shoaib, M., Ghias, M., Ali, N., Wahood, A., Shah, S.W.A., Shah, I., Shafiullah, Ghufran, M., & Rahman, M. (2017). Synthesis, docking studies and pharmacological activity of a synthetic flavonols. *Chiang Mai Journal of Science, 44*, 1-11.

Sichaem, J., Surapinit, S., Siripong, P., Khumkratok, S., Jong-aramruang, J., & Tip-pyang, S. (2010). Two new cytotoxic isomeric indole alkaloids from the roots of *Nauclea orientalis*. *Fitoterapia, 81*, 830-833.

Skalickova, S., Heger, Z., Krejcova, L., Pekarik, V., Bastl, K., Janda, J., … Kizek, R. (2015). Perspective of use of antiviral peptides against influenza virus. *Viruses, 7*, 5428-5442.

Sousa, S.F., Fernandes, P.A., and Ramos, M.J. (2006). Protein-ligand docking: Current status and future challenges. *PROTEINS: Structure, Function, and Bioinformatics*, *65*, 15-26.

Sousa, S.F., Fernandes, P.A., and Ramos, M.J. (2009). Molecular dynamics simulations on the critical states of the farnesyltransferase enzyme. *Bioorganic and Medicinal Chemistry, 17*, 3369-3378.

Sugimoto, H., Yamanishi, Y., Limura, Y., & Kawakami, Y. (2000). Donepezil hydrochloride (E2020) and other acetylcholinesterase inhibitors. *Current Medical Chemistry, 7*, 303-339.

Takayama, H., Tsutsumi, S., Kitajima, M., Santiarworn, D., Liawruangrath, B., & Aimi, N. (2003). Gluco-indole alkaloids from *Nauclea cadamba* in Thailand and transformation of 3α-dihydrocadambine into the indolopyridine alkaloid, 16-carbomethoxynaufoline. *Chemical and Pharmaceutical Bulletin, 51*, 232-233.

Takenaka, T. (2001). Classical vs reverse pharmacology in drug discovery. *BJU International, 88*, 7-10.

Tang, Y.T., & Marshall, G.R. (2011). Virtual screening for lead discovery. *Methods in Molecular Biology, 716*, 1-22.

Taylor, J.S., & Burnett, R.M. (2000). DARWIN: A program for docking flexible molecules. *Proteins, 41*, 173-191.

Trott, O., &Olson, A.J. (2010). AutoDock Vina: Improving the speed and accuracy of docking with a new scoring function, efficient optimization and multithreading. *Journal of Computational Chemistry, 31*, 455-461.

van der Schaar, H.M., Rust, M.J., Waarts, B-L., van der Ende-Metselaar, H., Kuhn, R.J., Wilschut, J., … Smit, J.M. (2007). Characterization of the early events in dengue virus cell entry by biochemical assays and single-virus tracking. *Journal of Virology, 81*, 12019-12028.

Vanquelef, E., Simon, S., Marquant, G., Garcia, E., Klimerak, G., Delepine, J.C., … Dupradeau, F.Y. (2011). R.E.D. Server: A web service for deriving RESP and ESP charges and building force field libraries for new molecules and molecular fragments. *Nucleic Acids Research, 39*, 23.

Venkatachalam, C.M., Jiang, X., Oldfield, T., & Waldman, M. (2003). LigandFit: A novel method for the shape-directed rapid docking of ligands to protein active sites. *Journal of Molecular Graphics and Modelling, 21*, 289-307.

Victório, C.P. (2011). Therapeutic value of the genus *Alpinia*, Zingiberaceae. *Brazilian Society of Pharmacognosy, 21*, 194-201.

Volk, D.E., Lee, Y-C., Li, X., Thiviyanathan, V., Gromowski, G.D., Li, L., … Gorenstein, D.G. (2007). Solution structure of the envelope protein domain III of dengue-4 virus. *Journal of Virology, 364*, 147-154.

von Itzstein, M., Wu, W.Y., Kok, G.B., Pegg, M.S., Dyason, J.C., Jin, B., … Penn, C.R. (1993). Rational design of potent sialidase-based inhibitors of influenza virus replication. *Nature, 363*, 418-423.

Wang, R., Lai, L., & Wang, S. (2002). Further development and validation of empirical scoring functions for structure-based binding affinity prediction. *Journal of Computer-Aided Molecular Design, 16*, 11-26.

Wang, J., Wolf, R.M., Kollman, P.A., & Case, D.A. (2004). Development and testing of a general Amber force field. *Journal of Computational Chemistry, 25*, 1157-1174.

Wang, C., Greene, D., Xiao, L., Qi, R., & Luo, R. (2018). Recent developments and applications of the MMPBSA method. *Frontiers in Molecular Biosciences*, *4*, 1-18.

Watterson, D., Kobe, B., & Young, P.R. (2012). Residues in domain III of the dengue virus envelope glycoprotein involved in cell-surface glycosaminoglycan binding. *Journal of General Virology, 93*, 72-82.

Weber, W., Hünenberger, P., & McCammon, J. (2000). Molecular dynamics simulations of a polyalanine octapeptide under Ewald boundary conditions: Influence of artificial periodicity on peptide conformation. *Journal of Physical Chemistry, B104*, 3668-4575.

Weiner, P.K., & Kollman, P.A. (1981). AMBER-assisted model building with energy refinement-A general program for modeling molecules and their interactions. *Journal of Computational Chemistry, 2*, 287-303.

Weiner, S.J., Kollman, P.A., Case, D.A., Singh, U.C., Ghio, C., Alagona, G., … Weiner, P. (1984). A new force-field for molecular mechanical simulation of nucleic-acids and proteins. *Journal of the American Chemical Society, 6*, 765-784.

Weiner, S.J., Kollman, P.A., Nguyen, D.T., & Case, D.A. (1986). An all-atom force field for simulations of protein and nucleic acids. *Journal of Computational Chemistry, 7*, 230-252.

Weng, G., Wang, E., Chen, F., Sun, H., Wang, Z., & Hou, T. (2019). Assessing the performance of MM/PBSA and MM/GBSA methods. 9. Prediction reliability of binding affinities and binding poses for protein–peptide complexes. *Physical Chemistry Chemical Physics, 21*, 10135-10145.

Whiting, D.R., Guariguata, L., Weil, C., & Show, J. (2011). IDF Diabetes Atlas: Global estimate of prevalence of diabetes for 2011 and 2030. *Diabetes Research and Clinical Practice, 94*, 311-332.

Wild, C., Oas, T., McDanal, C., Bolognesi, D., & Matthews, T. (1992). A synthetic peptide inhibitor of human immunodeficiency virus replication: Correlation between solution structure and viral inhibition. *Proceedings of the National Academy of Sciences of the United States of America, 89*, 10537-10541.

World Health Organization. (2017). Retrieved on July 23, 2017 from http://www.who.int/diabetes/en/.

World Health Organization. (2017). Retrieved on May 14, 2017 from http://www.who.int/denguecontrol/en/.

World Health Organization. Department of Noncommunicable Disease Surveillance. (1999). Definition, diagnosis and classification of diabetes mellitus and its complications: report of a WHO consultation. Part 1, Diagnosis and classification of diabetes mellitus. Geneva: World Health Organization. Retrieved on 24th July 2017 from http://www.who.int/iris/handle/10665/66040.

World Health Organization. (2019). Retrieved on February 1, 2020 from http://www.who.int/docs/default-source/wpro---documents/emergency/surveillance/dengue/dengue.

Wu, Y., Ding, Y., Tanaka, Y., & Zhang, W. (2014). Risk factors contributing to type 2 diabetes and recent advances in the treatment and prevention. *International Journal of Medical Sciences, 11*, 1185-1200.

Xu, Y., Rahman, N.A., Othman, R., Hu, P., & Huang, M. (2012). Computational identification of self-inhibitory peptides from envelope proteins. *Proteins, 80*, 2154-2168.

Yin, J., Bowen, D., & Southerland, W.M. (2006a). Barnase thermal titration via molecular dynamics simulations: Detection of early denaturation sites. *Journal of Molecular Graphics and Modelling, 24*, 233-243.

Yin, Z., Patel, S.J., Wang, W-L., Wang, G., Chan, W-L., Rao, K.R.R., … Keller, T.H. (2006b). Peptide inhibitors of dengue virus NS3 protease. Part 1: Warhead. *Bioorganic and Medicinal Chemistry Letters, 16*, 36-39.

Yoshioka, Y., Yoshimura, N., Matsumura, S., Wada, H., Hoshino, M., Makino, S., & Morimoto, M. (2019). α-glucosidase and pancreatic lipase inhibitory activities of diterpenes from indian mango ginger (*Curcuma amada* Roxb.) and its derivatives. *Molecules, 24*, 1-12.

Yunbao, L., & Muraleedharan, G.N., (2010). Labdane diterpenes in Curcuma mangga rhizomes inhibit lipid peroxidation,cyclooxygenase enzymes and human tumour cell proliferation. *Food Chemistry, 124*, 527-532.

Zanariah, H., Sri, W.T., Harvinder, K.G.S., & Winnie, C.S.S. (2015). Diabetes care in Malaysia: Problems, new models, and solutions. *Annals of Global Health, 81*, 851-862.

Zhang, L., Mohan, P.M., & Padmanabhan, R. (1992). Processing and localization of dengue virus type 2 polyprotein precursor NS3-NS4A-NS4B-NS5. *Journal of Virology, 66*, 7549-7554.

Zhang, Y., Zhang, W., Ogata, S., Clements, D., Strauss, J.H., Baker, T.S., … Rossmann, M.G. (2004). Conformational changes of the flavivirus E glycoprotein. *Structure, 12*, 1607-1618.

LIST OF PUBLICATIONS AND PAPER PRESENTED

LIST OF PUBLICATION

Isa, D.M., Chin, S.K., Chong, W.L., Zain, S.M., Rahman, N.A., & Lee, V.S. (2018). Dynamics and binding interactions of peptide inhibitors of dengue virus entry. *Journal of Biological Physics*, *45*, 63-76.

PAPER PRESENTED

Isa, D.M., Chin, S.K., Chong, W.L., Zain, S.M., Rahman, N.A., & Lee, V.S. (2015). *Integrated in silico techniques for exploiting the bioactive compounds of antiviral*. Paper presented at the 10th International Conferences on the Physical Properties and Application of Advanced Materials, 17-21st November 2015, Chiang Mai, Thailand.